Metabolite plasticity drives carbon-nitrogen resource budgeting to enable division of labor in a clonal community.

Sriram Varahan[1], Vaibhhav Sinha[2,3], Adhish Walvekar[1], Sandeep Krishna[2] and Sunil Laxman[1*]

[1]InStem - Institute for Stem Cell Science and Regenerative Medicine, Bangalore 560065.

[2]Simons Centre for the Study of Living Machines, National Center for Biological Sciences, Bangalore 560065.

[3]Manipal Academy of Higher Education, Manipal 576104.

*Correspondence: sandeep@ncbs.res.in , sunil@instem.res.in

Abstract:

Previously, we discovered that in glucose-limited yeast colonies, metabolic constraints drive cells into groups exhibiting gluconeogenic and glycolytic metabolic states. Here, threshold amounts of trehalose - a limiting, produced resource, controls the emergence and self-organization of the cells exhibiting the glycolytic state, by acting as a carbon source to fuel these metabolic demands (Varahan et al., 2019). We now discover that the plasticity of use of a non-limiting resource, aspartate, controls both resource production and the emergence of heterogeneous cell states, based on differential cellular metabolic budgeting. In gluconeogenic cells, aspartate provides carbon for trehalose production, while in glycolytic cells using trehalose for carbon, aspartate supplies nitrogen to drive nucleotide synthesis. This metabolic plasticity of aspartate enables carbon-nitrogen budgeting, thereby driving the biochemical self-organization of distinct cell states. Through this organization, cells in each state exhibit true division of labor, providing bet-hedging and growth/survival advantages for the whole community.

Introduction:

During the development of microbial communities, groups of cells come together and exhibit heterogeneity within spatial organization (Ackermann 2015). As the community develops, cells can present specialization of function, which allows the community as a whole to perform various tasks including the acquisition of food, defense against competing microorganisms, or more efficient growth (Newman, 2016; Niklas, 2014; West and Cooper, 2016). This division of labor allows breakdown of complex biological processes into simpler steps, eliminating the need for individual cells to perform several tasks simultaneously, thereby enhancing the overall efficiency with which cells in the community function (Giri et al., 2019; David R. Johnson et al., 2012; Rueffler et al., 2012; van Gestel et al., 2015). Due to these advantages, division of labor is widely prevalent across diverse microbial communities and can be found at different levels of biological organization (Gordon, 2016; Kirk, 2003; Tarnita et al., 2013). However, the underlying rules that enable division of labor within cell populations remain to be deciphered.

In particular, microbial community development is commonly triggered by nutrient limitation (Ackermann, 2015; Hoehler and Jørgensen, 2013; Johnson et al., 2012). Clearly, an optimal allocation of resources is critical for maximizing overall fitness within a microbial community, especially when the availability of nutrients is limiting. One strategy by which the community can manage the requirement of different resources is by sharing metabolic products, and this is employed by many microbial communities (D'Souza et al., 2018; Liu et al., 2015). Since resources can often be insufficient, the sharing of such resources might incur a cost to the cell. Hence, different cells of the community exhibit metabolic interdependencies, presumably to balance out trade-offs arising from resource sharing. While this concept has been demonstrated for example, in synthetically engineered systems, where required metabolic dependencies are created between non-isogenic cells (Campbell et al., 2016, 2015), this has been exceptionally challenging to demonstrate within a clonal community of cells. We recently

47 discovered that metabolic constraints are sufficient to enable the emergence and maintenance of cells
48 in specialized biochemical states within a clonal yeast community (Varahan et al., 2019). Remarkably,
49 this occurs through a simple, self-organized biochemical system. In yeast growing in low glucose, cells
50 are predominantly gluconeogenic. As the colony matures, groups of cells exhibiting glycolytic
51 metabolism emerge with spatial organization. Strikingly, this occurs through the production (via
52 gluconeogenesis) and accumulation of a limiting metabolic resource, trehalose. As this resource builds
53 up, some cells spontaneously switch to utilizing trehalose for carbon, which then drives a glycolytic
54 state. This also depletes the resource, and therefore a self-organized system of trehalose producers and
55 utilizers establish themselves, enabling structured phenotypic heterogeneity (Varahan et al., 2019).

56 This observation raises a deeper question, of how such groups of heterogeneous cells can sustain
57 themselves in this self-organized biochemical system. In particular, is it sufficient to only have the build-
58 up of this limiting, controlling resource? How are carbon and nitrogen requirements balanced within the
59 cells in the heterogeneous states? In this study, we uncover how a non-limiting resource with plasticity
60 in function can control the organization of this entire system. We find that the amino acid aspartate,
61 through distinct use of its carbon or nitrogen backbone, enables the emergence and organization of
62 heterogeneous cells. In gluconeogenic cells, aspartate is utilized in order to produce the limiting carbon
63 resource, trehalose, which in turn is utilized by other cells that switch to and stabilize in a glycolytic
64 state. Combining biochemical, computational modeling and analytical approaches, we find that
65 aspartate is differentially utilized by the oppositely specialized cells of the community as a carbon or a
66 nitrogen source to sustain different metabolism. This carbon/nitrogen budgeting of aspartate is crucial
67 for the emergence of distinct cell states in this isogenic community. Through this, cells groups show
68 complete division of labor, and each specialized state provides distinct proliferation and survival
69 advantages to the colony. Collectively, we show how the carbon/nitrogen economy of a cell community

enables a self-organizing system based on non-limiting and limiting resources, which creates organized phenotypic heterogeneity in cells.

Results:

Amino acid driven gluconeogenesis is critical for emergence of metabolic heterogeneity:

In a previous study (Varahan et al., 2019), we discovered that trehalose controls the emergence of spatially organized, metabolically heterogeneous groups of cells within a yeast colony growing in low glucose. Within this colony were cells with high gluconeogenic activity, and other cells showing high glycolytic/pentose phosphate pathway (PPP) activity (**Figure 1A**). The high glycolytic/PPP activity cells could be distinguished as 'light' cells, and the highly gluconeogenic cells as 'dark', based purely on optical density as observed by brightfield microscopy, as shown in **Figure 1A** (Varahan et al., 2019). In this system, cells start in a gluconeogenic state, and these cells (dark) produce trehalose. When a threshold concentration of external trehalose is reached, a subpopulation of cells switch to trehalose consumption that drives a glycolytic state, and these cells continue to proliferate as light cells (**Figure 1A**). Trehalose is a limiting resource since it is not freely available in the glucose limited external environment, and must be synthesized via gluconeogenesis (François et al., 1991). We therefore first asked how the loss of gluconeogenesis affects the emergence of metabolically specialized light cells. For this, we genetically generated mutants that lack two key gluconeogenic enzymes (PCK1 and FBP1). These gluconeogenic mutants (*Δpck1* and *Δfbp1*) expectedly formed smooth colonies completely lacking structured morphology (which correlates with the absence of metabolic heterogeneity)(**Figure 1B and Figure 1-figure supplement 1A**). Further, these mutants had essentially undetectable cells with high PPP activity (light cells), based on the fluorescence-signal of a PPP reporter, as compared to a wild-type colony, although the total number of viable cells in all the colonies were comparable (**Figure 1C and**

Figure 1-figure supplement 1B). This confirms that gluconeogenesis is critical for the emergence and maintenance of metabolic heterogeneity in the colony.

Trehalose, the produced resource controlling the switch to the light state (Varahan et al., 2019), is a disaccharide made up of two molecules of glucose and is produced via gluconeogenesis. This two-state community of cells requires a continuous supply of trehalose to sustain itself. Therefore, in order to address how dark cells maintained threshold concentrations of trehalose, we asked how this resource itself is produced. Notably, the media conditions under which these colonies develop essentially have non-limiting amounts of amino acid resources (2% yeast extract and 2% peptone). We therefore hypothesized that amino acids (available in non-limiting levels) could act as carbon sources (via possible anaplerotic processes) to fuel trehalose production in dark cells. We tested this by growing wild-type cells in media devoid of free amino acids, but with sufficient ammonium sulfate (Minimal media). Wild-type colonies failed to develop structured colonies (which correlates with the lack of metabolic heterogeneity) in the absence of free amino acids, and this could be rescued by adding back amino acids to this media (**Figure 1D**). Expectedly, this amino acid dependent rescue of colony morphology depended on gluconeogenesis, since a *Δpck1* strain failed to develop morphology even after the addition of amino acids to the medium (**Figure 1D**). This shows that non-limiting amino acids promote the development of structured colonies exhibiting metabolic heterogeneity, in a gluconeogenesis dependent manner. Interestingly this amino acid dependent effect is very specific. In add-back experiments in minimal medium, amongst all amino acids tested, aspartate supplementation strongly promoted the development of structured colonies exhibiting metabolic heterogeneity, more robustly than the addition of any other amino acids individually or in combination (**Figure 1D and Figure 1-figure supplement 1C**). This was validated by experiments wherein wild-type colonies that developed in minimal media, supplemented either with all amino acids, or only aspartate alone, exhibited spatially restricted metabolic heterogeneity comparable to the wild-type colonies grown in rich media. The light

117 cell population was estimated using the fluorescent PPP reporter, which serves as an excellent proxy for
118 light cells (Varahan et al., 2019) (**Figure 1E and Figure 1-figure supplement 1B**). Collectively, these
119 results reveal that aspartate is essential for the development of metabolically specialized colonies in a
120 gluconeogenesis-dependent manner.

121

122 **Aspartate promotes light cell emergence by directly fueling trehalose synthesis:**

123 In contrast to their canonical roles as nitrogen sources, amino acids can also act as carbon donors for
124 several metabolic processes (Boyle, 2005). While amino acids can enter the tricarboxylic acid (TCA) cycle
125 *via* anaplerosis, and TCA intermediates in turn can enter gluconeogenesis, aspartate is unique. It is the
126 only amino acid that can directly enter gluconeogenesis, without feeding into the TCA cycle. This is by
127 conversion of aspartate into oxaloacetate directly in the cytosol. All the other amino acids have to be
128 first transported to the mitochondria and enter the TCA cycle, and these TCA intermediates must then
129 be transported back to the cytosol to enter gluconeogenesis (Brunengraber and Roe, 2006). Since the
130 addition of aspartate alone to minimal media was sufficient for light cells to emerge, we tested if
131 aspartate is a direct carbon source required for trehalose production within the colony, since trehalose
132 is a pre-requisite for light cell emergence. Wild-type colonies were grown in minimal media
133 supplemented with all amino acids, or aspartate alone, or all amino acids without aspartate (aspartate
134 dropout) and total trehalose levels in the 7-day old colonies were measured. As controls, trehalose
135 levels in the *Δpck1* colonies (gluconeogenesis defective) and *Δtps1* colonies (trehalose synthesis
136 defective) were measured. Compared to colonies grown in minimal medium, colonies grown in minimal
137 medium supplemented with all amino acids, or aspartate alone, had significantly higher amounts of
138 trehalose (**Figure 2A**). Notably, the level of trehalose in wild-type colonies grown in aspartate dropout
139 minimal medium was significantly lower compared to colonies grown in minimal media supplemented

with all amino acids or just aspartate, demonstrating that aspartate can be the primary carbon contributor towards trehalose synthesis (**Figure 2A**). As expected, *Δpck1* colonies (gluconeogenesis defective) and *Δtps1* (trehalose synthesis defective) had background levels of trehalose (**Figure 2A**). Furthermore, colonies grown on aspartate dropout medium had fewer light cells (quantified using the PPP reporter activity) compared to colonies grown in minimal media supplemented with all amino acids or just aspartate (**Figure 2B and Figure 2-figure supplement 1**). This shows that aspartate enables trehalose production, which in turn controls the emergence of metabolic heterogeneity in these clonal colonies (**Figure 2A & 2B**). To demonstrate that aspartate directly provides the carbon backbone of trehalose, we grew colonies in minimal medium (low glucose) supplemented with ^{13}C-labeled aspartate, and measured intracellular levels of ^{13}C–labeled gluconeogenic intermediates or end-products directly by targeted mass spectrometric methods described earlier (Vengayil et al., 2019)(**Figure 2C**). Cells in wild-type colonies accumulated ^{13}C-labeled 3-phosphoglycerate (3-PG) and ^{13}C-labeled trehalose, while these labeled metabolites were undetectable in a gluconeogenic mutant (*Δpck1*) (**Figure 2D**). Collectively, these data show that aspartate provides the carbon skeleton for trehalose production *via* gluconeogenesis, and this turn is essential for the emergence of spatially restricted metabolic heterogeneity.

An agent-based model suggests how differential aspartate utilization drives the emergence of self-organized, metabolically heterogeneous states:

We had previously noted that the light cells had higher rates of nucleotide synthesis (Varahan et al., 2019). Synthesis of the nucleotide backbone requires an assimilation of carbon (typically from glucose derived metabolites, notably pentose sugars from the PPP), as well as nitrogen that comes from amino acids (primarily glutamine and aspartate) (Boyle, 2005). Indeed, this donation of nitrogen by aspartate

163 towards nucleotide synthesis is considered a primary role of this amino acid. Interestingly, within the
164 dark cells of the colony, aspartate is used as a carbon source for the synthesis of trehalose (Figure 2D).
165 We therefore hypothesized that distinct cells in the colony might differentially utilize aspartate
166 predominantly as either a carbon or a nitrogen source. This raises the central idea of molecular
167 budgeting: how is the utilization of aspartate as a carbon/nitrogen source managed in different types of
168 cells? To theoretically address this question, we refined our originally coarse-grained mathematical
169 model from (Varahan et al., 2019). In the original model that simulates the development of the colony
170 with dark and light cells, the resource driving the emergence of light cells was featureless and could only
171 be used to drive hypothetically opposite metabolism (Varahan et al., 2019). In our new model, we now
172 build-in molecule specificity. Based on experimental data, we incorporate aspartate utilization for the
173 emergence of metabolic subpopulations, as well as differential growth rates, and self-organization
174 within the colony. The processes now included in the model are explained below (See Materials and
175 Methods for a detailed description):

176 Both dark and light cells utilize externally available resources to synthesize and accumulate the
177 metabolites needed for growth. We can now assign two specific categories for these accumulating
178 metabolites: carbon (C) and nitrogen (N). The dark cells utilize a single resource, aspartate, to serve both
179 C and N requirements. Aspartate itself is a molecule that is in excess in the environment (non-limiting).
180 We propose that the dark cells budget the aspartate flux for both these requirements, and some of the
181 accumulated C (as trehalose) becomes available in the extracellular environment. From our earlier
182 findings (Varahan et al., 2019), we know that the extracellular trehalose controls when some dark cells
183 switch to being light cells. The light cells utilize the available trehalose for their C needs (driving
184 glycolysis and the PPP). However, aspartate remains readily available for their N requirements, which
185 includes nucleotide synthesis (this is illustrated in the model schematic and sample colony in **Figure 3A**).
186 We now implement this revised model as an agent-based simulation, and monitor colony growth with

these new assumptions of aspartate utilization. The specific modifications from the original model and the **new parameters** are introduced below:

(i) Both light and dark **[cell blocks]** take up aspartate from the external environment at the same rate. Light cells can also take up trehalose from the surroundings. If the maximum amount of trehalose taken up per time step is Cmax, the rate of aspartate uptake is **AspU***Cmax.

(ii) Dark cells budget the aspartate utilization for different ends. A fraction, '**f**' is utilized for nitrogen (N) needs, the remainder, (1-f), is utilized for carbon (C) needs.

(iii) The aspartate to C conversion requires a yield coefficient, **Y**, because aspartate is a 4-carbon molecule and trehalose (from gluconeogenesis) is a larger molecule (12-carbon). Three molecules of aspartate will therefore be required to make one molecule of trehalose.

(iv) A fraction, **Pf**, of this accumulated C inside dark cell blocks is secreted into the extracellular environment as trehalose. Thus, we can couple the trehalose production by dark cells to their aspartate consumption and utilization. Additionally, there will be an imposed upper limit to this secreted amount, but for our simulation this extra constraint is not limiting to cells (see **Figure 3–figure supplement 1**).

(v) In the new model, the two cell types (dark and light) accumulate both C and N to a minimum amount before division. We assume that dark and light cell [blocks] need the same minimum amount of C, normalized to a value of 1.0 units. However, the light cell blocks have different N requirements, due to a higher rate of nucleotide synthesis (as observed in (Varahan et al., 2019)). Hence, while the dark cell blocks have a minimum N requirement normalized to 1.0, the light cells need **ExN***1.0. Once cells accumulate the minimum amount, the probability of division for both cell types are the same. See Table 3 for values of these parameters and see **Figure 3–figure supplement 2** for a comparison of the division rate of the dark and light cells.

By varying the two main parameters in this study, the model makes the following predictions:

1. More of the aspartate taken up by dark cells is allocated for carbon metabolism and trehalose synthesis

We vary the fraction of the aspartate flux allocated to nitrogen, **f**, from 0.0-1.0 (0% - 100%) only in the dark cells. The colonies formed from some selected values are shown in **Figure 3B** to show the general trend. Low values of 'f' generate virtual colonies which are similar to experimental ones. As the value of f increases, enough resource cannot be allocated to fulfil carbon requirements for light cells to divide.

2. Aspartate uptake rate by both types of cells is higher than the rate of uptake of trehalose by light cells

The parameter **AspU** dictates the relative rate of aspartate uptake compared to trehalose uptake rate by light cells. Dark cells take up aspartate at the same rate as light cells. However, in dark cells, aspartate is responsible for carbon metabolism and trehalose generated in the system. Varying this parameter as shown in Figure 3C, we see that if the rate of uptake for aspartate is the same as the uptake rate for trehalose (AspU = 1.0), the colonies cannot grow like the wild-type colony (**Figure 3B**). This can be attributed to the fact that 4 molecules of aspartate are required for the synthesis of 1 molecule of trehalose. Hence it will be impossible for cells to synthesize sufficient amounts of trehalose required for the emergence of light cells, if the uptake rate of aspartate by dark cells is equal to the uptake of trehalose by light cells. Therefore, in simple simulations, a higher value of AspU (= 4.0) provides enough carbon for the dark cells despite budgeting, to synthesize trehalose (C for light cells in the model) that is required for the proliferation of light cells. Since aspartate drives the growth of both dark and light cells in a direct and indirect manner, larger values of AspU give larger colonies and vice versa, as shown in **Figure 3C**. Also see **Figure 3–figure supplements 3, 4** and **5** and **Videos: 1-4**.

Aspartate allows differential carbon/nitrogen budgeting in light and dark cells of the colony *in vivo*:

In our model, we now observe that carbon/nitrogen budgeting of aspartate by the dark cells is critical for the emergence of light cells. We previously showed that light cells exhibit high PPP activity and nucleotide biosynthesis, using carbon precursors derived from the trehalose, provided by the dark cells (Varahan et al., 2019). As mentioned earlier, aspartate serves a nitrogen donor in the synthesis of purine and pyrimidine nucleotides and serves as a carbon donor in the synthesis of trehalose (**Figure 4A**) (Jones, 1980). Based both on theory and our model simulations, can we now experimentally test if aspartate predominantly serves as a carbon source in dark cells to fuel trehalose production, while primarily providing nitrogen for nucleotide biosynthesis in light cells? We decided to investigate this directly, by using a stable-isotope based metabolic-flux approach. We grew wild-type colonies in minimal media containing ^{13}C-labeled aspartate, and collected light and dark cells by rapid micro-dissection of the ~1 cm colonies, followed by immediate quenching of the cells and metabolite extraction (see Materials and methods), and measured the amounts of ^{13}C–labeled gluconeogenic metabolites (3PG and ^{13}C–trehalose), respectively in dark and light cells by LC-MS/MS. Dark cells accumulated significantly higher levels of ^{13}C-labeled 3-PG and ^{13}C-labeled trehalose as compared to the light cells (**Figure 4B**). Using a similar experimental approach with ^{15}N-labeled aspartate provided, we next measured the relative nitrogen-label incorporation into nucleotides in light and dark cells. Here, in stark contrast to the earlier results for carbon, the light cells accumulated substantially higher levels of ^{15}N-labeled nucleotides compared to dark cells (**Figure 4C**). Collectively, we experimentally demonstrate differential C/N budgeting in light and dark cells, based on aspartate utilization.

Thus, aspartate exhibits metabolite plasticity within the cells of a colony. The gluconeogenic dark cells utilize this amino acid primarily as a carbon source (for trehalose production), while the light cells (with high PPP activity) primarily utilize aspartate as a nitrogen donor for nucleotide biosynthesis.

Collectively, these results reveal how plasticity in the use of a non-limiting resource, aspartate, enables the development of metabolically heterogeneous colonies.

Dark and light cells exhibit division of labor, with distinct survival and collective growth advantages:

What can this type of formation of specialized states, derived from biochemically self-organizing systems, mean for such a community of cells? Non-genetic heterogeneity can be beneficial for cell populations. Due to heterogeneity, some individual cells can survive environmental changes, which thereby allow genotypes to persist in ever-changing environments. Further, division of labor between individuals of a community can enhance collective community growth, development, and the efficiency of the functions that they perform (Giri et al., 2019; van Gestel et al., 2015). We therefore wondered if the distinct metabolic states within the yeast colony conferred a collective growth or survival advantage. Yeast cells routinely encounter environmental fluctuations like desiccation and freezing/thawing regularly (Gasch, 2007; Gasch and Werner-Washburne, 2002). Here, trehalose particularly enables the survival of yeast cells when faced with such environmental insults (D'Amore et al., 1991; Erkut et al., 2016; Wiemken, 1990). Since dark (gluconeogenic) cells accumulate high amounts of trehalose (Varahan *et al*., 2019), we suspected that these cells might better survive extreme conditions like desiccation and freezing/thawing. To test this, we isolated light and dark cells from ~7-day old colonies and subjected them to repeated freeze/thaw cycles or severe desiccation (7 and 14 days). We used yeast cells grown in glycolytic or gluconeogenic liquid medium as controls, and measured cell survival either by spotting the cells on a fresh plate (for a freeze/thaw tolerance) or counting the percentage of surviving cells (for desiccation tolerance). Dark cells showed markedly higher survival rates post freeze/thaw treatment (similar to the gluconeogenic control) compared to light cells (which phenocopied cells grown in high

277 glucose) (**Figure 5A**). Similarly, dark cells survived complete desiccation better than light cells (**Figure**
278 **5B**). Finally, we looked at the role of dark cells in the long-term survivability of the wild-type colony as a
279 whole. To dissect this, we used cells lacking the trehalase enzyme (*Δnth1*) as a control since colonies
280 from these cells produce but cannot utilize trehalose to fuel glycolysis, and lack light cells (Varahan *et*
281 *al*., 2019). We also compared these to the long-term survivability of *Δpck1* cells (gluconeogenesis-
282 defective), since these colonies lack both light and dark cells. Although we did not see a difference in the
283 number of viable cells in the 7-day old colonies, in mature (21-day) colonies the percentage of viable
284 cells were significantly lower in the *Δpck1* colonies compared to the wild-type and *Δnth1* colonies
285 (**Figure 5C**). Therefore, the presence of dark cells positively influences the long-term survivability of the
286 colony as a whole, and these cells can survive environmental insults like desiccation, freeze/thaw cycles
287 and nutrient limitation.

288 Complex colony development under nutrient limitation includes foraging responses, where the outward
289 expansion of the colony allows the cells to reach fresh nutrient sources (Palková and Váchová, 2016;
290 Váchová and Palková, 2018). We previously observed that light cells enable efficient colony expansion,
291 and colonies with only dark cells (*Δnth1* trehalase mutants) cannot expand as efficiently as a wild-type
292 colony (Varahan et al., 2019). Since the gluconeogenesis defective mutant (*Δpck1*) lacked light cells, we
293 also hypothesized that these colonies are compromised at colony expansion as well. To test this, wild-
294 type, *Δnth1* and *Δpck1* were spotted as colonies and colony expansion was monitored over time (7 days
295 and 21 days). At 21 days, the *Δnth1* and *Δpck1* colonies had significantly reduced expansion compared to
296 wild-type colonies. This reiterates that the light cells are important for the effective long-term expansion
297 of the colony (**Figure 5D & 5E**). This also suggests the possibility that colonies lacking light cells may not
298 be able to expand towards suitable nutrients. To contextualize this with the localized availability of high-
299 quality nutrients, we designed an experiment where an external source of glucose was added to the
300 plate at some distance from the colony, and the expansion of colonies towards this glucose source was

estimated (**Figure 5F**). Strikingly, the light cells from wild-type colonies showed rapid, directional proliferation towards the glucose source. Notably, both the *Δnth1* cells (trehalose-breakdown deficient, no light cells), and the *Δpck1* cells (no trehalose production) showed markedly reduced directional movement towards the glucose source (**Figure 5F**). This was quantified using an expansion factor (the ratio of the colony area of the half of the colony growing towards the glucose source/ colony area of the other half of the colony) (**Figure 5F)**. These data conclusively show that light cells are essential for the outward expansion and foraging response of the colony. Together, the presence of dark and light cells allows greater colony survival, resistance to stress, and the ability to expand towards preferred nutrient sources.

Discussion:

We present a model illustrating how plasticity in the use of a non-limiting resource, aspartate, is critical for the emergence and maintenance of spatially organized, distinct metabolic states of groups of cells. Aspartate is required for gluconeogenic cells to achieve threshold concentrations of a limiting resource, trehalose, which in turn drives specialization in these clonal microbial communities (**Figure 6**). In low glucose conditions, cells expectedly perform gluconeogenesis to replenish glucose reserves. During this process, cells utilize aspartate predominantly as a carbon source that drives gluconeogenesis. One eventual metabolic outcome of gluconeogenesis is trehalose synthesis, and cells accumulate synthesized trehalose. Trehalose also directly benefits gluconeogenic cells, allowing them to survive environmental stresses including desiccation and repeated freeze/thaw cycles. As threshold concentrations of trehalose available externally are reached, some cells stochastically take up and consume trehalose, breaking it down to glucose. This uptake and consumption of trehalose switches the metabolic state of these cells to that of high PPP/Glycolysis. In this complimentary metabolic state, cells now utilize aspartate as a

nitrogen source. The combination of available glucose (from trehalose) combined with the use of aspartate as a nitrogen source allows light cells to synthesize end point molecules like nucleotides, which enable rapid proliferation, and efficient expansion and foraging for nutrients.

Our previous study showed how trehalose availability can create a self-organized system, where some cells will switch a new (glycolytic) metabolic state, and these cells will themselves be sustained by the cells in the original (gluconeogenic) metabolic state that produce trehalose (Varahan et al., 2019). Such an idea of threshold amounts of sentinel metabolites that can control cell states is an emerging area of interest (Cai and Tu, 2011; Krishna and Laxman, 2018). In this study, we take a step back, to discover how such a self-organizing system can emerge by using a metabolically plastic resource, aspartate. In order for cells to achieve threshold levels of the limiting, controlling resource, trehalose, cells utilize a non-limiting resource (aspartate) to fuel trehalose biosynthesis. Conventionally, aspartate is only thought of as a 'nitrogen' source since it is required for nucleotide metabolism (Boyle, 2005). However, as we observe in this study, aspartate serves as an effective carbon source to synthesize trehalose via gluconeogenesis in dark cells. Notably, in light cells, when carbon becomes non-limiting (via trehalose utilization), aspartate can go back to its 'conventional' role as a nitrogen donor for nucleotide synthesis. This differential use of a single metabolite to meet distinct carbon and nitrogen demands of cell in opposite metabolic states is a remarkable example of metabolic budgeting within spatially organized cells. This plastic ability of aspartate, combined with non-limiting amounts at which it is available makes it the driver of phenotypic heterogeneity in this system.

The principles emerging from this two-state system in a yeast colony are pertinent to the emergence of complexity from relatively simple processes. In an elegant theoretical framework, Cornish-Bowden and Cardenas formulated how in a living system, self-organizing processes can maintain themselves indefinitely, and how they can be modified across generations (Cornish-Bowden and Cárdenas, 2008). In their study, they extend the original idea of *'metabolism-replacement systems'* (M-R systems), and the

348 importance of metabolic closure (Rosen, 1972, 1966, 1965). A living M-R system, as conceptualized
349 (Cornish-Bowden and Cárdenas, 2008), requires a few specific properties: (1) some molecules are
350 available in unlimited quantities from the environment, (2) a partition must be present to separate the
351 system from its environment, (3) these molecules can enter in and out of the partition, (4) the chemistry
352 of these molecules enable them to participate in biochemical cycles, (5) these molecules/reactions will
353 not participate in processes that interfere with these biochemical cycles, and (6) the thermodynamics of
354 these reactions are sufficiently favorable. By these definitions, this yeast colony where the combination
355 of aspartate in (practically) non-limiting amounts, as well as the build-up and use of a limiting resource
356 (trehalose), along with the separation of compartments (and cells) for different biochemical processes
357 where these molecules are used, largely works as a *M-R* system that enables the stable emergence and
358 maintenance of phenotypically heterogeneous states. This system, with biochemical specialization and
359 division of (metabolic) labor is also a demonstration of both the importance of specific enzymes (eg.
360 trehalase), and metabolic control analysis, leading to the distribution of tasks via the differential
361 budgeting of carbon and nitrogen. This is the essence of a cellular or multi-cellular economy where
362 metabolic supply and demand must be balanced, and which depends on the combination of resources
363 available (Hofmeyr, 2008; Hofmeyr and Cornish-Bowden, 2000).

364 The result of this self-organized system are groups of clonal cells, spatially organized into groups that
365 exhibit division of labor (West and Cooper 2016, Kolter 2015). Dividing tasks between lower units (such
366 as groups of cells) can allow tremendous enhancements in efficiency of processes. By enforcing division
367 of labor, microbial communities effectively achieve what multicellular organisms do within tissues, and
368 aid in the development of the whole community. While division of labor has often been used loosely,
369 more stringent definitions of division of labor require (1) functional complementarity, (2) synergistic
370 advantages, (3) negative frequency-dependent selection, and (4) positive assortment (Giri et al., 2019).
371 This yeast colony, with its self-organized system of cells in opposite metabolic states, appears to satisfy

372 these criteria for division of labor. The result is a community of clonal cells where each
373 metabolic/phenotypic state has individual advantages (greater survival or greater proliferation), enables
374 the colony to bet-hedge the best condition for growth and survive adversity, and also provides an
375 increased growth advantage and capability to forage for new nutrients.

376 Summarizing, we demonstrate how efficient carbon/nitrogen resource budgeting and metabolic
377 plasticity of a non-limiting resource controls the emergence of spatially separated cells in specialized
378 states. This division of labor provides collective advantages to the community to survive environmental
379 challenges and expand towards new resources, in a manner reminiscent of multicellular organisms.

380

381 **Experimental Procedures:**

382 Yeast strains and growth media:

383 The natural, prototrophic sigma 1278b strain (referred to as wild-type or WT) was used in all
384 experiments. Strains with gene deletions or chromosomally tagged proteins (at the C-terminus) were
385 generated as described (Longtine et al., 1998). Strains used in this study are listed in Table 1. The growth
386 medium used in this study is rich medium (1% yeast extract, 2% peptone and 2% glucose or 0.1%
387 glucose).

388 Colony spotting assay:

389 All strains were grown overnight at 30˚C in either rich medium or defined minimal medium, as specified.
390 5 microliters of the overnight cultures were spotted on rich medium (low glucose) (1% yeast extract, 2%
391 peptone, 0.1% glucose and 2% agar) or minimal medium (low glucose) (0.67% yeast nitrogen base with
392 ammonium sulfate, without amino acids and 2% agar) supplemented with either all amino acids, all

amino acids excluding aspartate or just aspartate at a concentration of 2mM. Plates were incubated at 30˚C for 7 days unless mentioned otherwise.

Colony imaging:

For observing colony morphology, colonies were imaged using SZX-16 stereo microscope (Olympus) wherein the light source was above the colony. Bright-field imaging of 7-day old colonies were done using SZX-16 stereo microscope (Olympus) wherein the light source was below the colony. Epifluorescence microscopy imaging of 7-day old gluconeogenesis reporter colonies (pPCK1-mCherry), pentose phosphate pathway (PPP) reporter colonies (pTKL1-mCherry) and *HXK1* reporter colonies (pHXK1-mCherry) were imaged using the red filter (excitation of 587 nm, emission of 610 nm) of SZX-16 stereo microscope (Olympus).

Biochemical estimation of trehalose/glycogen levels:

Trehalose and glycogen from yeast samples were quantified as described previously, with minor modifications (Gupta and Laxman, 2020). 10 OD_{600} of light cells and dark cells from 7-day old wild-type colonies (rich medium, 0.1% glucose) were collected. After re-suspension in water, 0.5 ml of cell suspension was transferred to 4 tubes (2 tubes for glycogen assay and the other 2 tubes for trehalose assay). When sample collections were complete, cell samples (in 0.25 M sodium carbonate) were boiled at 95–98°C for 4 hr, and processed as described earlier (Gupta and Laxman, 2020) to estimate steady state trehalose amounts, based on glucose release. Assays were done using a 96-well plate format. Samples were added into each well with appropriate dilution within the dynamic range of the assay (20–80 µg/ml glucose). For the measurement of extracellular trehalose measurement, a single wild-type colony (1-day to 7-day old colony) was re-suspended in 100 microliters of water and centrifuged at 20000g for 5 min. The supernatant was collected and buffered to a pH of 5.4 (optimal for trehalase activity) using sodium acetate buffer (pH 5.0), and subsequently trehalose was estimated using the same

416 protocol.

417 Freeze-thaw survival assay:

418 Light cells and dark cells were isolated from 7-day old wild-type colonies and washed twice with water.
419 Subsequently cells were resuspended at an OD_{600} of 0.1. These were subjected to rapid freezing by
420 plunging tubes into liquid nitrogen, followed by thawing at room temperature, for multiple cycles. 5 µl
421 from each of these samples were spotted onto rich medium plates. Cells were allowed to grow for 18
422 hours before imaging the plates and estimating survival.

423

424 Desiccation tolerance assay:

425 Desiccation tolerance assays were performed as described earlier (Erkut et a(Gupta and Laxman, 2020)l.,
426 2016), with slight modifications. Briefly, light and dark cells were isolated from 7-day old wild-type
427 colonies and brought to a final volume of 1 ml in PBS. Two hundred microliter aliquots were transferred
428 to a 96- well tissue culture plate, centrifuged, and the excess water was removed. Cells were allowed to
429 desiccate in a humid incubator at 27˚C for 7 days or 14 days. Samples were resuspended in diluted PBS
430 to a final volume of 200 µl and plated for colony counting. The number of colony forming units per
431 milliliter (cfu/ml) for each plate was measured, using an average from three independent controls. The
432 relative viability of each experimental sample (done in biological triplicate) was determined by dividing
433 the cfu/ml for that sample by the average cfu/ml of the control plates.

434 Glucose foraging assay:

435 Wild-type, Δ*nth1* and Δ*pck1* cells were grown overnight and 5 µl were spotted onto rich, low glucose
436 medium. A small paper disc was soaked in 50% glucose solution overnight and placed at a distance of

2cm from the colony spots. Colonies were allowed to develop at 30˚C for 7 days and imaged. As a control, strains were spotted on a plate containing paper disc soaked in PBS.

Metabolite extractions and measurements by LC-MS/MS:

Light cells and dark cells isolated from wild-type colonies grown in different media were rapidly harvested and metabolites were extracted as described earlier (Walvekar et al., 2018). Metabolites were measured using LC-MS/MS method as described earlier (Walvekar et al., 2018). Standards were used for developing multiple reaction monitoring (MRM) methods on Sciex QTRAP 6500. Metabolites were separated using a Synergi 4µ Fusion-RP 80A column (100 × 4.6 mm, Phenomenex) on Agilent's 1290 infinity series UHPLC system coupled to the mass spectrometer. For positive polarity mode, buffers used for separation were- buffer A: 99.9% H_2O/0.1% formic acid and buffer B: 99.9% methanol/0.1% formic acid (Column temperature, 40°C; Flow rate, 0.4 ml/min; T = 0 min, 0% B; T = 3 min, 5% B; T = 10 min, 60% B; T = 11 min, 95% B; T = 14 min, 95% B; T = 15 min, 5% B; T = 16 min, 0% B; T = 21 min, stop). For negative polarity mode, buffers used for separation were- buffer A: 5 mM ammonium acetate in H_2O and buffer B: 100% acetonitrile (Column temperature, 25°C; Flow rate: 0.4 ml/min; T = 0 min, 0% B; T = 3 min, 5% B; T = 10 min, 60% B; T = 11 min, 95% B; T = 14 min, 95% B; T = 15 min, 5% B; T = 16 min, 0% B; T = 21 min, stop). The area under each peak was calculated using AB SCIEX MultiQuant software 3.0.1.

^{15}N- and ^{13}C- based metabolite labelling experiments:

For detecting ^{15}N label incorporation in nucleotides, ^{15}N Ammonium sulfate (Sigma-Aldrich) and ^{15}N Aspartate (Cambridge Isotope Laboratories) with all nitrogen atoms labeled were used. For ^{13}C-labeling experiment, ^{13}C aspartate with all carbon atoms labeled (Cambridge Isotope Laboratories) was used. All the parent/product masses measured are enlisted in Table 2. For all the nucleotide measurements, release of the nitrogen base was monitored in positive polarity mode. For all sugar phosphates, the

phosphate release was monitored in negative polarity mode. The HPLC and MS/MS protocol was similar to those explained above.

Model Methods and Parameters:

Model construction

We extend the coarse-grained model from (Varahan et al., 2019) to include the idea that both dark and light cells need to accumulate enough N and C for cell division. Once again, the model consists of a population of dark and light "cell blocks" on a 2D grid. In addition, the model also There is another grid of the same shape and size which tracks spatiotemporal levels of extracellular trehalose on this grid as it is secreted, consumed and diffuses. We do not track the levels of aspartate in the environment as it is assumed to be a non-limiting resource.

Initial conditions of the model

We start with an approximately circular colony 20 grid lengths in radius at the center of our grid. 95-99% of the 1257 cell blocks are in the dark state. There is no extracellular trehalose on the trehalose grid at the start.

Model implementation

Running the model is almost identical to the implementation in (Varahan et al., 2019), except for a few extra steps, refinements, and parameters to consider. For clarity, we will outline the entire algorithm here using default parameter values. The following steps are to be carried out in each time step after colony initialization.

A) If a block at the location (x,y) is dark then:
1. If the trehalose levels at (x,y) are above a certain threshold $\mathbf{T_{DL}}$ = 1.5 units, then the dark cell block can switch to being a light cell block with a probability $\mathbf{P_{DL}}$ = 0.5.
2. If the block is still dark, consume **AspU*Cmax= 4 * 0.05** units of aspartate.

3. Allocate a fraction, **f = 0.125** of the consumed aspartate towards an internal nitrogen (N) pool
4. Convert the remaining (1-f) = 0.875 fraction of the aspartate to carbon (C) with a yield coefficient **Y= 0.31.**
5. From the internal pool of C, secrete a fraction **Pf = 0.049** into the extracellular space as trehalose at the location (x,y). This secreted amount has an upper limit of **0.12** units of trehalose per unit t/Time
6. If both the internal levels of C and N are greater than or equal to 1.0 unit,s then the dark cell can divide with a probability of **g=0.04.**
7. If the block can divide, then check if there is an empty location in the immediate neighborhood. The immediate neighborhood is the set of locations {(x-1,y), (x + 1,y), (x,y-1), (x,y + 1)}.
8. If there is at least one empty space, preferably divide into an empty location that has more occupied neighbors; if not, pick randomly an empty location to divide into. After division, the two daughter blocks are each assigned half the internal C & N reserves of the original mother cell block.

B) If the block at the location (x,y) is light then:

1. If the trehalose levels at (x,y) are below a certain threshold $\mathbf{T_{LD} = 10^{-4}}$ units, the light cell block can switch to dark with a probability $\mathbf{P_{LD} = 10^{-4}}$ (also see Figure 3 – figure supplement 4 for comparison with the model from Varahan et al., 2019).
2. If the block is still light, consume all the trehalose at its location up to a maximum of **Cmax = 0.05** units and add to an internal C pool.
3. Consume **AspU*Cmax = 4*0.05** units of aspartate and add to an internal N pool.
4. If internal levels of C are greater than 1.0 unit,s and internal levels of N are greater than **Exn = 4.0** units, then the light cell block can divide with a probability **g = 0.04**.
5. If the block can divide, then check if there is an empty location in the immediate neighborhood. The immediate neighborhood is the set of locations {(x-1,y), (x + 1,y), (x,y-1), (x,y + 1)}.
6. If there is at least one empty space, preferably divide into an empty location that has more occupied neighbors; if not, pick randomly an empty location to divide into. After division, the two daughter blocks are each assigned half the internal C & N reserves of the original mother cell block.

C) After every time step, update the trehalose concentrations on the grid by implementing 2D diffusion using the FTCS scheme identical to the one used in (Varahan et al., 2019).

The above algorithm and parameter values simulate a wild type colony as seen in Figure 3A. For variations of the two main parameters, **f** and **AspU**, refer to Figure 3B & C and for a more detailed picture, refer to Figure 3–figure supplement 3. The set of parameters used in the model is shown in table 3 and for a flowchart of the algorithm, refer to Figure 3–figure supplement 5.

Model parameters

The new parameters introduced in the current model are chosen to reliably reproduce patterns similar to the experimental WT colony (both the final form, as well as at different stages of its growth).

1. The parameter '**f**' is the fraction of aspartate that a dark cell block allocates towards nitrogen needs. Its default value is 0.125.
2. The parameter '**AspU**' controls the relative influx of aspartate compared to the influx of trehalose. We argue that since aspartate is a much smaller molecule, it has a higher flux compared to trehalose for the light cells. Both light and dark cell blocks take up aspartate at this same rate. Its default value is 4.0.
3. Conversion of aspartate to carbon necessitates a yield factor, '**Y**'. We use a value of 0.31 as it gives us a better pattern.
4. This model links aspartate consumption to trehalose production. The aspartate is converted and adds to a growing internal C pool. A small fraction of this pool is secreted/leaked into the extracellular environment. This fraction '**Pf**' is 0.049.
5. In addition, we put an upper limit on the absolute amount of trehalose secreted by a dark cell block in a time step. This is set at 0.12 units. This was inserted to prevent a large amount of trehalose being secreted by a dark cell block if it had not divided for several time steps. However, in our simulations, we find that only a negligible fraction of the cell blocks are operating at this limit (see Figure 3–figure supplement 1)
6. Light cells are observed to divide faster than dark cells and have higher rates of nucleotide synthesis. So, we propose that they have higher nitrogen requirements compared to the dark cells. We use the scaling parameter '**ExN'** to account for this. We set the default value of this parameter to 4.0.

Code availability

We implemented the model using Python and Jupyter Notebooks. The code used in this study is available at: https://github.com/vaibhhav/metabplastic

Acknowledgements:

This work was supported by a Wellcome Trust-DBT India Alliance Intermediate Fellowship (IA/I/14/2/501523) and institutional support from inStem and the Department of Biotechnology (DBT), Govt. of India to SL, a Wellcome Trust-DBT India Alliance Early Career Fellowship (IA/E/16/1/502996) to SV, institutional support from NCBS-TIFR and the Simons Foundation to VS and SK. VS and SK acknowledge support of the Department of Atomic Energy, government of India, under project no. 12-R&D-TFR-5.04-0800. We acknowledge the extensive use of the NCBS/inStem/CCAMP mass spectrometry facility.

References:

Ackermann M. 2015. A functional perspective on phenotypic heterogeneity in microorganisms. *Nat Rev Microbiol* **13**:497–508. doi:10.1038/nrmicro3491.

Boyle J. 2005. Lehninger principles of biochemistry (4th ed.): Nelson, D., and Cox, M. *Biochem Mol Biol Educ*. doi:10.1002/bmb.2005.494033010419.

Brunengraber H, Roe CR. 2006. Anaplerotic molecules: Current and future. *J Inherit Metab Dis*. doi:10.1007/s10545-006-0320-1.

Campbell K, Vowinckel J, Mülleder M, Malmsheimer S, Lawrence N, Calvani E, Miller-Fleming L, Alam MT, Christen S, Keller MA, Ralser M. 2015. Self-establishing communities enable cooperative metabolite exchange in a eukaryote. *Elife* **4**. doi:10.7554/eLife.09943.

Campbell K, Vowinckel J, Ralser M. 2016. Cell-to-cell heterogeneity emerges as consequence of metabolic cooperation in a synthetic yeast community. *Biotechnol J* **11**:1169–78. doi:10.1002/biot.201500301.

Cornish-Bowden A, Cárdenas ML. 2008. Self-organization at the origin of life. *J Theor Biol*. doi:10.1016/j.jtbi.2007.07.035.

D'Amore T, Crumplen R, Stewart GG. 1991. The involvement of trehalose in yeast stress tolerance. *J Ind Microbiol*. doi:10.1007/BF01575882.

D'Souza G, Shitut S, Preussger D, Yousif G, Waschina S, Kost C. 2018. Ecology and evolution of metabolic cross-feeding interactions in bacteria. *Nat Prod Rep* **35**:455–488. doi:10.1039/c8np00009c.

Erkut C, Gade VR, Laxman S, Kurzchalia T V. 2016. The glyoxylate shunt is essential for desiccation tolerance in C. Elegans and budding yeast. *Elife*. doi:10.7554/eLife.13614.

François J, Neves MJ, Hers HG. n.d. The control of trehalose biosynthesis in Saccharomyces cerevisiae: evidence for a catabolite inactivation and repression of trehalose-6-phosphate synthase and trehalose-6-phosphate phosphatase. *Yeast* **7**:575–87. doi:10.1002/yea.320070605.

Gasch AP. 2007. The environmental stress response: a common yeast response to diverse environmental stressesYeast Stress Responses. doi:10.1007/3-540-45611-2_2.

Gasch AP, Werner-Washburne M. 2002. The genomics of yeast responses to environmental stress and starvation. *Funct Integr Genomics*. doi:10.1007/s10142-002-0058-2.

Giri S, Waschina S, Kaleta C, Kost C. 2019. Defining Division of Labor in Microbial Communities. *J Mol Biol*. doi:10.1016/j.jmb.2019.06.023.

Gordon DM. 2016. From division of labor to the collective behavior of social insects. *Behav Ecol Sociobiol*. doi:10.1007/s00265-015-2045-3.

Gupta R, Laxman S. 2020. Steady-state and Flux-based Trehalose Estimation as an Indicator of Carbon Flow from Gluconeogenesis or Glycolysis. *BIO-PROTOCOL*. doi:10.21769/bioprotoc.3483.

Hoehler TM, Jørgensen BB. 2013. Microbial life under extreme energy limitation. *Nat Rev Microbiol*. doi:10.1038/nrmicro2939.

Hofmeyr JHS. 2008. The harmony of the cell: The regulatory design of cellular processes. *Essays Biochem*. doi:10.1042/BSE0450057.

Hofmeyr JHS, Cornish-Bowden A. 2000. Regulating the cellular economy of supply and demand. *FEBS Lett*. doi:10.1016/S0014-5793(00)01668-9.

Johnson David R., Goldschmidt F, Lilja EE, Ackermann M. 2012. Metabolic specialization and the assembly of microbial communities. *ISME J*. doi:10.1038/ismej.2012.46.

599 Johnson David R, Goldschmidt F, Lilja EE, Ackermann M. 2012. Metabolic specialization and the assembly
600 of microbial communities. *ISME J* **6**:1985–91. doi:10.1038/ismej.2012.46.

601 Jones ME. 1980. Pyrimidine Nucleotide Biosynthesis in Animals: Genes, Enzymes, and Regulation of UMP
602 Biosynthesis. *Annu Rev Biochem*. doi:10.1146/annurev.bi.49.070180.001345.

603 Kirk DL. 2003. Seeking the ultimate and proximate causes of Volvox multicellularity and cellular
604 differentiationIntegrative and Comparative Biology. doi:10.1093/icb/43.2.247.

605 Liu J, Prindle A, Humphries J, Gabalda-Sagarra M, Asally M, Lee DD, Ly S, Garcia-Ojalvo J, Süel GM. 2015.
606 Metabolic co-dependence gives rise to collective oscillations within biofilms. *Nature* **523**:550–4.
607 doi:10.1038/nature14660.

608 Newman SA. 2016. “Biogeneric” developmental processes: drivers of major transitions in animal
609 evolution. *Philos Trans R Soc Lond B Biol Sci* **371**. doi:10.1098/rstb.2015.0443.

610 Niklas KJ. 2014. The evolutionary-developmental origins of multicellularity. *Am J Bot* **101**:6–25.
611 doi:10.3732/ajb.1300314.

612 Palková Z, Váchová L. 2016. Yeast cell differentiation: Lessons from pathogenic and non-pathogenic
613 yeasts. *Semin Cell Dev Biol* **57**:110–119. doi:10.1016/j.semcdb.2016.04.006.

614 Rosen R. 1972. Autonomous state classifications by dynamical systems. *Math Biosci*. doi:10.1016/0025-
615 5564(72)90015-6.

616 Rosen R. 1966. A note on replication in (M, R)-systems. *Bull Math Biophys*. doi:10.1007/BF02476988.

617 Rosen R. 1965. Some comments on re-estalishability. *Bull Math Biophys*. doi:10.1007/BF02477257.

618 Rueffler C, Hermisson J, Wagner GP. 2012. Evolution of functional specialization and division of labor.
619 *Proc Natl Acad Sci U S A*. doi:10.1073/pnas.1110521109.

620 Tarnita CE, Taubes CH, Nowak MA. 2013. Evolutionary construction by staying together and coming
621 together. *J Theor Biol*. doi:10.1016/j.jtbi.2012.11.022.

622 Váchová L, Palková Z. 2018. How structured yeast multicellular communities live, age and die? *FEMS*
623 *Yeast Res* **18**. doi:10.1093/femsyr/foy033.

624 van Gestel J, Vlamakis H, Kolter R. 2015. Division of Labor in Biofilms: the Ecology of Cell Differentiation.
625 *Microbiol Spectr*. doi:10.1128/microbiolspec.mb-0002-2014.

626 Varahan S, Walvekar A, Sinha V, Krishna S, Laxman S. 2019. Metabolic constraints drive self-organization
627 of specialized cell groups. *Elife*. doi:10.7554/elife.46735.

628 Vengayil V, Rashida Z, Laxman S. 2019. The E3 ubiquitin ligase Pib1 regulates effective gluconeogenic
629 shutdown upon glucose availability. *J Biol Chem*. doi:10.1074/jbc.RA119.009822

630 Walvekar A, Rashida Z, Maddali H, Laxman S. 2018. A versatile LC-MS/MS approach for comprehensive
631 quantitative analysis of central metabolic pathways [version 1; referees: 2 approved]. *Wellcome*
632 *Open Res. doi:10.12688/wellcomeopenres.14832.1.*

633 West SA, Cooper GA. 2016. Division of labor in microorganisms: An evolutionary perspective. *Nat Rev*
634 *Microbiol*. doi:10.1038/nrmicro.2016.111.

635 Wiemken A. 1990. Trehalose in yeast, stress protectant rather than reserve carbohydrate. *Antonie Van*
636 *Leeuwenhoek*. doi:10.1007/BF00548935

637

638

639

640

641 **Table 1.** Strains and plasmids used in this study.

642

Strain/genotype	Information	Source/reference
Wild-type (WT)	YBC16G1, prototrophic sigma1278b, *MAT*a	Isolate *via* Fink Lab
WT *(pTKL1-mCherry)*	*Wild-type strain with pentose phosphate pathway reporter plasmid (mCherry with TKL1 promoter)*	(Varahan et al., 2019)
Δpck1	*MAT a pck1::kanMX6*	this study
Δfbp1	*MAT a fbp1::kanMX6*	this study
Δnth1	*MAT a nth1::kanMX6*	(Varahan et al., 2019)
Δpck1 (pTKL1-mCherry)	*Δpck1 strain with pentose phosphate pathway reporter plasmid (mCherry with TKL1 promoter)*	this study
Δfbp1 (pTKL1-mCherry)	*Δfbp1 strain with pentose phosphate pathway reporter plasmid (mCherry with TKL1 promoter)*	this study
Plasmid	**Information**	**Source/reference**
pTKL1-mCherry	*mCherry under the TKL1 promoter and CYC1 termin-ator. p417 centromeric plasmid backbone, G418^R.*	(Varahan et al., 2019)

643

644

645

646

647

648

649

650

651

652 **Table 2.** Mass transitions used for LC-MS/MS experiments.

Nucleotides	Formula	Parent/Product (positive polarity)	Comment (for ^{15}N experiment)
AMP	$C_{10}H_{14}N_5O_7P$	348/136	Product has all N
15N_AMP_1		349/137	
15N_AMP_2		350/138	
15N_AMP_3		351/139	
15N_AMP_4		352/140	
15N_AMP_5		353/141	
GMP	$C_{10}H_{14}N_5O_8P$	364/152	Product has all N
15N_GMP_1		365/153	
15N_GMP_2		366/154	
15N_GMP_3		367/155	
15N_GMP_4		368/156	
15N_GMP_5		369/157	
CMP	$C_9H_{14}N_3O_8P$	324/112	Product has all N
15N_CMP_1		325/113	
15N_CMP_2		326/114	
15N_CMP_3		327/115	
UMP	$C_9H_{13}N_2O_9P$	325/113	Product has all N
15N_UMP_1		326/114	
15N_UMP_2		327/115	
Trehalose and sugar phosphates	**Formula**	**Parent/Product (negative polarity)**	**Comment (for ^{13}C experiment)**
Trehalose	$C_{12}H_{22}O_{11}$	341.3/179.3	
13C_Trehalose_12		353.3/185.3	Product has 6 C all of which are labeled
13C_3PG_3		188/97	
G6P	$C_6H_{13}O_9P$	259/97	Monitoring the phosphate release
13C_G6P_6		265/97	
6PG	$C_6H_{13}O_{10}P$	275/97	Monitoring the phosphate release

653

654

655

656

657

658

659

660 **Table 3.** Model parameters.

Main parameters	Notation	Default Value	Range of Variation
Fraction of aspartate flux allocated to N in dark cell blocks	f	0.125	0.0 - 1.0 (0-100%)
Relative rate of aspartate uptake compared to trehalose uptake rate	AspU	4.0	0.0-8.0
Additional parameters			
Yield (converting N to C)	Y	0.31 C/N	
Fraction secreted as trehalose, per dark cell block	Pf	0.049 /Time	--
Max secreted trehalose, per dark cell block	--	0.12 units/Time	--
Extra N for light cells	ExN	4.0	--
Aspartate consumed by dark and light cell blocks	AspU*Cmax	0.2/Time	
Parameters from previous model			
Growth rate (light and dark cell block)	g	0.04/Time	--
Max trehalose consumed by a light cell block	Cmax	0.05 units/Time	
Switching threshold (dark to light)	T_{DL}	1.5 units	--
Switching probability (dark to light)	P_{DL}	0.5/Time	
Switching threshold (light to dark)	T_{LD}	0.0001 units	
Switching probability (light to dark)	P_{LD}	0.0001/Time	
Scaled diffusion constant of trehalose	D_{eff}	0.24 L^2/Time	

661

662

663

664

665

666

667

668

669

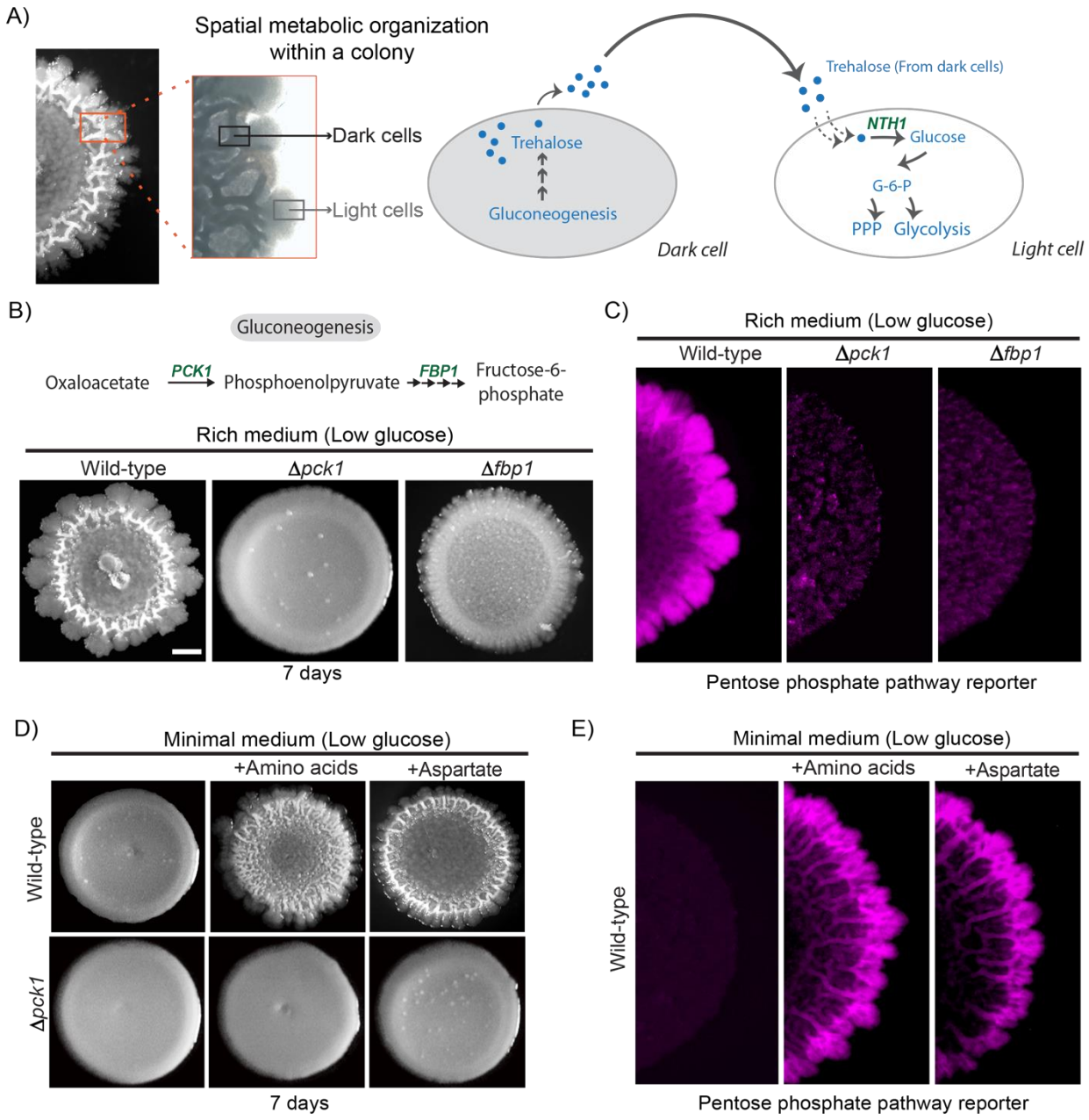

Figure 1. Amino acid driven gluconeogenesis is critical for emergence of phenotypic heterogeneity:

(A) External trehalose controls the emergence of light cells. Trehalose synthesized by the dark cells fuels glycolysis and pentose phosphate pathway in light cells.

(B) Gluconeogenesis is required for development of structural morphology in the colonies. The panel shows the morphology of mature wild-type and gluconeogenic mutants (Δ*pck1* and Δ*fbp1*) yeast colonies in rich medium, with supplemented glucose as the sole variable. Scale bar: 2 mm. Also see Figure 1-figure supplement 1A for more information.

679 **(C)** Spatial distribution of mCherry fluorescence across a colony, indicating the activity of a reporter for
680 pentose phosphate pathway (*TKL1*) activity in wild-type and gluconeogenesis defective mutants (Δ*pck1*
681 and Δ*fbp1*).

682 **(D)** Amino acids and in particular aspartate is required for the development of structural morphologies in
683 the colonies in a gluconeogenesis dependent manner. The panel shows the morphology of mature wild-
684 type and gluconeogenesis-defective (Δ*pck1*) yeast colonies in minimal medium (low glucose), with and
685 without amino acid supplementation, or with only aspartate supplementation.

686 **(E)** Spatial distribution of mCherry fluorescence across a colony, indicating the activity of a reporter for
687 pentose phosphate pathway (*TKL1*) activity in wild-type colonies grown either in minimal media or
688 minimal media supplemented with all amino acids or just aspartate.

689

690

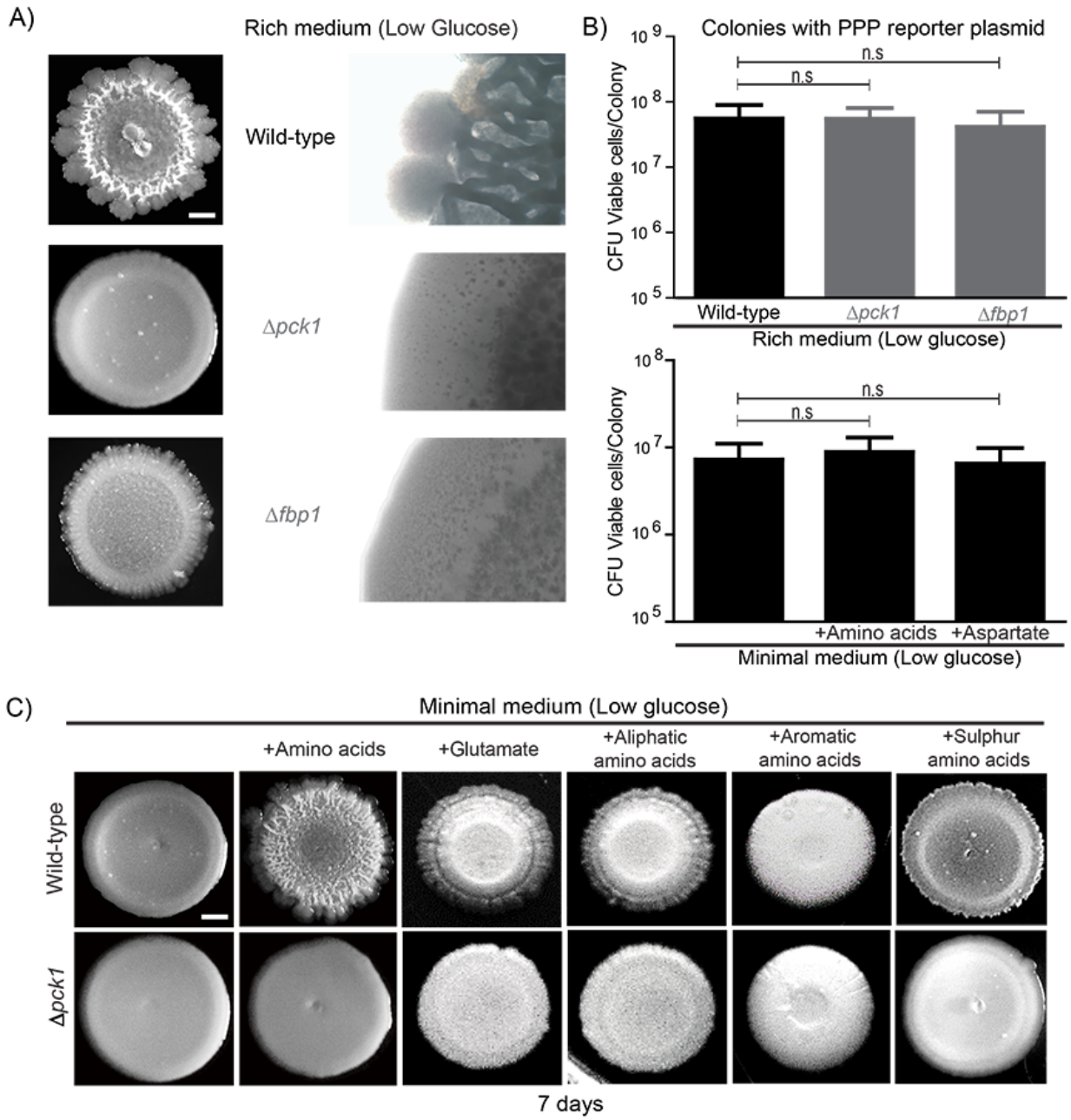

691

692 **Figure 1-figure supplement 1:**

693 **(A)** Gluconeogenesis is required for development of structural morphology in the colonies. The panel
694 shows the morphology of mature wild-type and gluconeogenic mutants (Δ*pck1* and Δ*fbp1*) yeast colonies
695 in rich medium, with supplemented glucose as the sole variable. Scale bar: 2 mm.

696 **(B)** Viability of cells in wild-type, Δ*pck1* and Δ*fbp1* colonies grown in rich medium (low glucose) for 7 days
697 were measured by collecting cells from the colonies and plating them in rich medium (n=5). Statistical
698 significance was calculated using unpaired t test and error bars represent standard deviation. Similarly,
699 viability of cells in wild-type colonies grown either in minimal media or minimal media supplemented with
700 all amino acids, or just aspartate, were measured by collecting cells from the colonies and plating them in

rich medium (n=5). Statistical significance was calculated using unpaired t test and error bars represent standard deviation.

(C) The panel shows the morphology of mature wild-type and gluconeogenesis defective (Δ*pck1*) yeast colonies grown for 7 days in minimal medium (low glucose), with and without supplementation of the indicated amino acids. Scale bar: 2 mm.

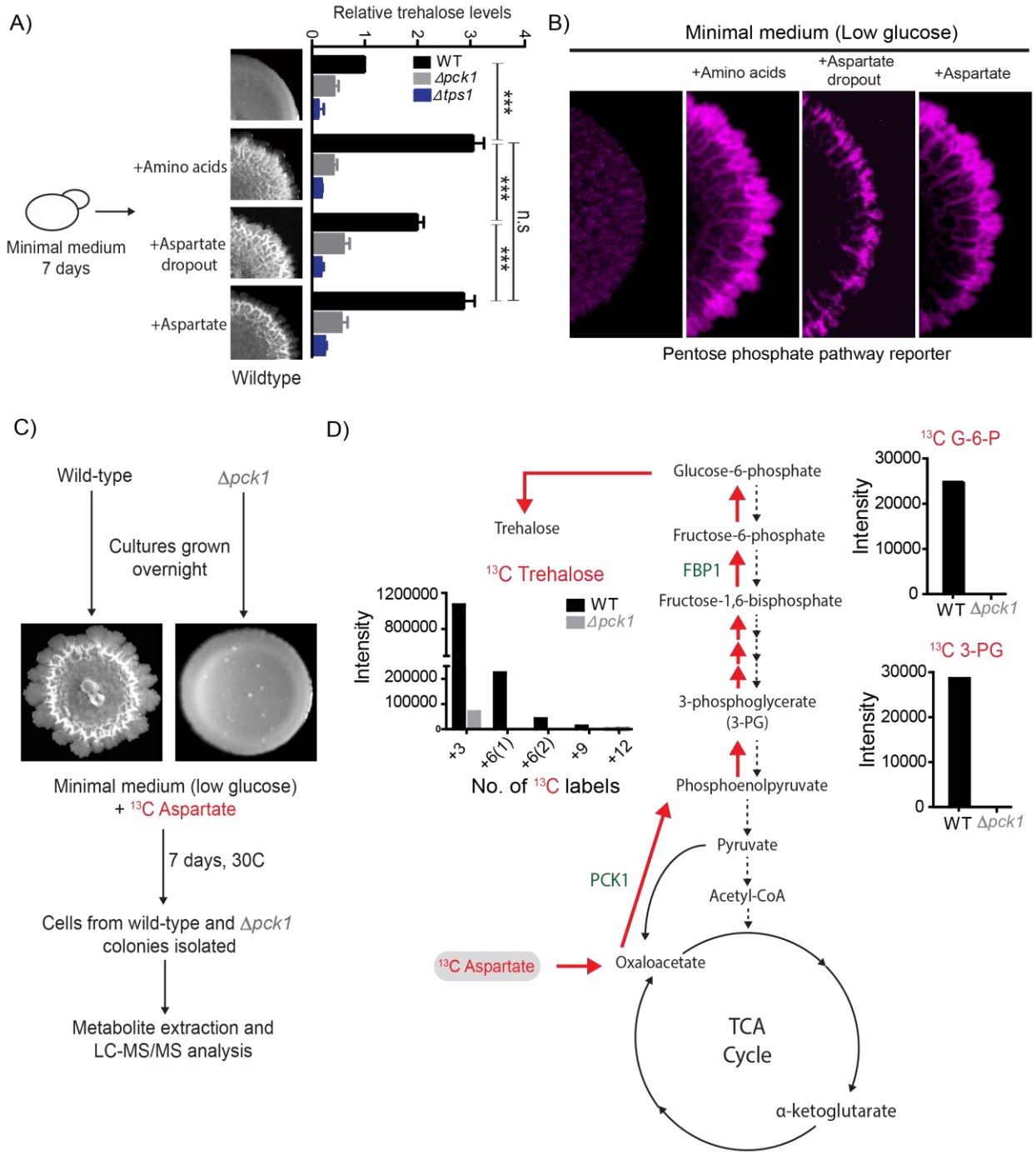

Figure 2. Aspartate enables light cell emergence by fueling trehalose synthesis:

(A) Comparative steady-state amounts of trehalose measured in wild-type, Δ*pck1* (gluconeogenesis defective) and Δ*tps1* (trehalose synthesis defective) colonies grown in minimal medium, or minimal medium supplemented with either all amino acids, or aspartate alone, or all amino acids without aspartate (aspartate dropout) (n=3). Colony insets represent wild-type colony morphology in different media conditions. Statistical significance was calculated using unpaired t test (*** indicates $p<0.001$) and error bars represent standard deviation.

(B) Aspartate significantly contributes to colony development and emergence of light cells. Spatial distribution of mCherry fluorescence across a colony, indicating the activity of a reporter for pentose phosphate pathway (*TKL1*) activity in wild-type yeast colonies grown in minimal medium (low glucose), supplemented with either all amino acids, or aspartate alone, or all amino acids without aspartate (aspartate dropout). Also see Figure 2-figure supplement 1A for more information.

(C) Comparative metabolic-flux based analysis comparing ^{13}C incorporation from ^{13}C-labeled aspartate into newly synthesized gluconeogenic intermediates (3-phosphoglycerate and Glucose-6-phosphate) and trehalose, in wild-type and *pck1* deletion colonies.

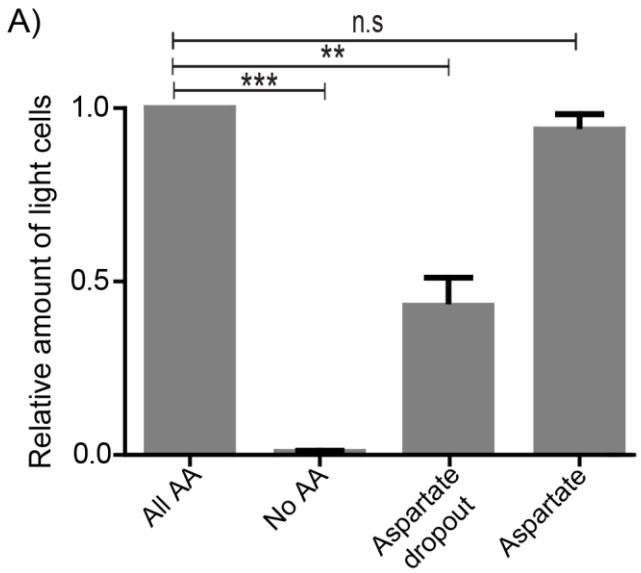

Figure 2-figure supplement 1:

(A) The light cell population was calculated by spotting wild-type cells harboring the PPP reporter plasmid either in minimal media or minimal media supplemented with either all amino acids or aspartate or all amino acids without aspartate (aspartate dropout). After 7 days of growth, cells from the entire colony (for each media condition) were collected and the percentage of fluorescent cells from colonies grown in each media condition were quantified (2000 cells per colony and 3 colonies per media condition). Statistical significance was calculated using unpaired t test (** indicates $p<0.01$, *** indicates $p<0.001$) and error bars represent standard deviation.

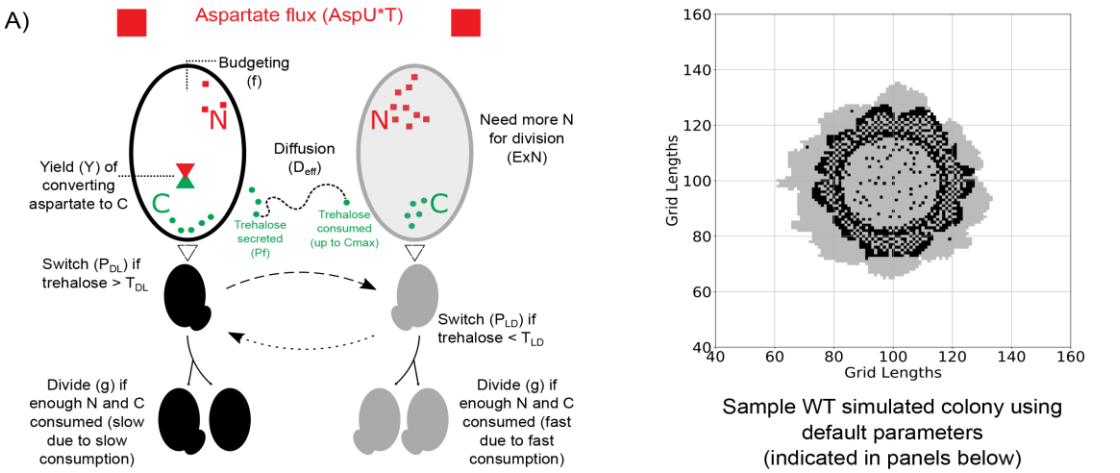

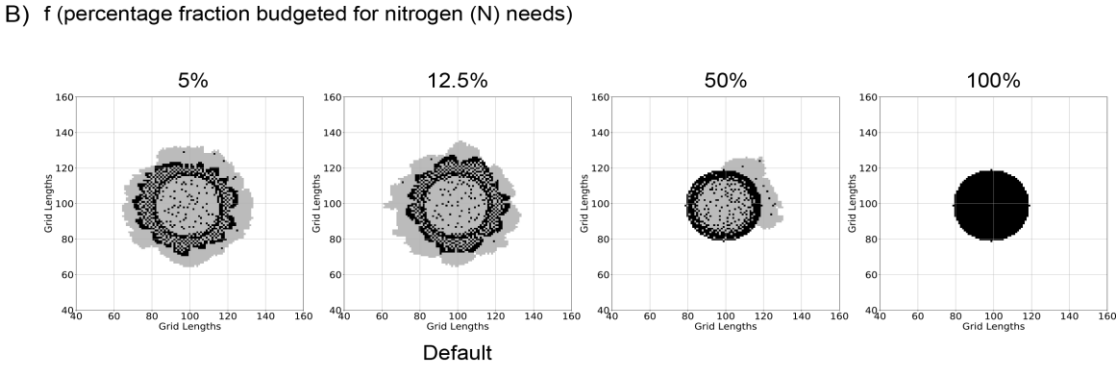

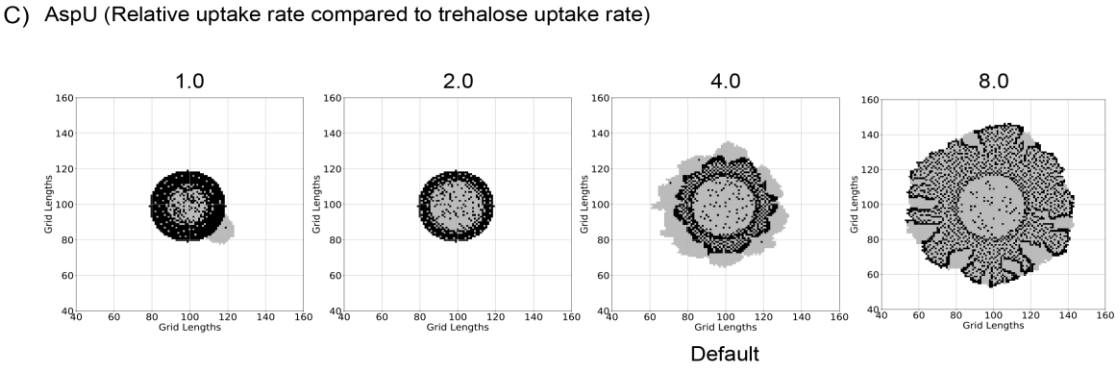

740

741 **Figure 3. An agent-based model for carbon-nitrogen budgeting reveals principles of metabolic**
742 **heterogeneity via self-organization:**

743 **(A)** A model schematic based on an experimental understanding of aspartate utilization by the two cell
744 types in the system. Dark and light cells are colored accordingly. Dark cells take in aspartate, budget it for
745 nitrogen (N) and carbon (C) needs. Some of the accumulating C is secreted into the extracellular
746 environment as trehalose, triggering the switching into light cells and also acting as the primary C source
747 for light cells as it diffuses in the 2D space. On the right, we have a sample simulated colony generated
748 from a default parameter set. Parameters are indicated in the parentheses.

(B) Varying the fraction of aspartate flux allocated towards nitrogen (N) in order to observe the simulated colony over the same length of time. When the majority of the flux is used for carbon (C) needs, the simulated colonies resemble experimental ones. If less aspartate is allocated for C rather than N, the developed colonies no longer resemble the experimental colonies.

(C) Varying the relative rate of aspartate uptake compared to trehalose uptake by the light cells in order to observe simulated colonies over the same length of time. If the rate is the same, as shown in the first simulated colony where AspU=1.0, the colony is underdeveloped. A middle value of AspU=4.0 generates colonies similar to experimental colonies, while for a large value of AspU on the right, the dark cell blocks and light cell blocks have similar division times and the final colony is larger.

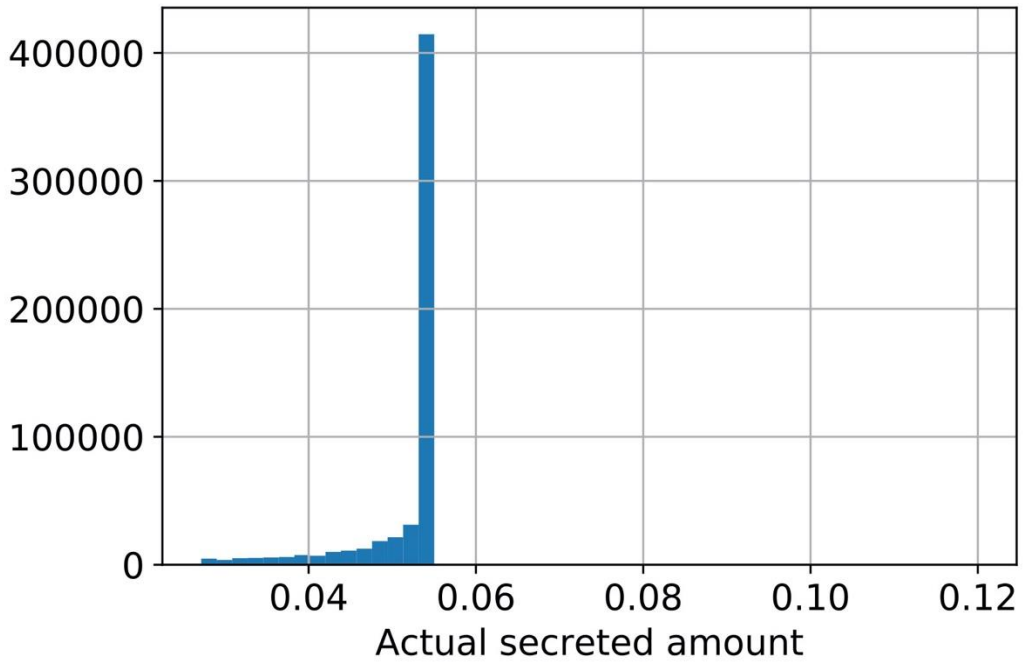

Figure 3-figure supplement 1: A histogram of the amount of trehalose secreted per unit time per dark cell throughout a simulation. Dark cells secrete a fraction, Pf, of their internal carbon levels as trehalose. However, we place an upper limit on the absolute amount of secreted trehalose at 0.12 units/Time. This limit is meant to mimic realistic export conditions. An assumption made is that due to physiological constraints on the cell, the amount of trehalose exported/present outside should not be arbitrarily large. This figure shows that most of the time, the cells are operating well below this upper limit. This demonstrates that the rate of trehalose production in the system is governed by other processes of the model pertaining to uptake, budgeting and growth by division.

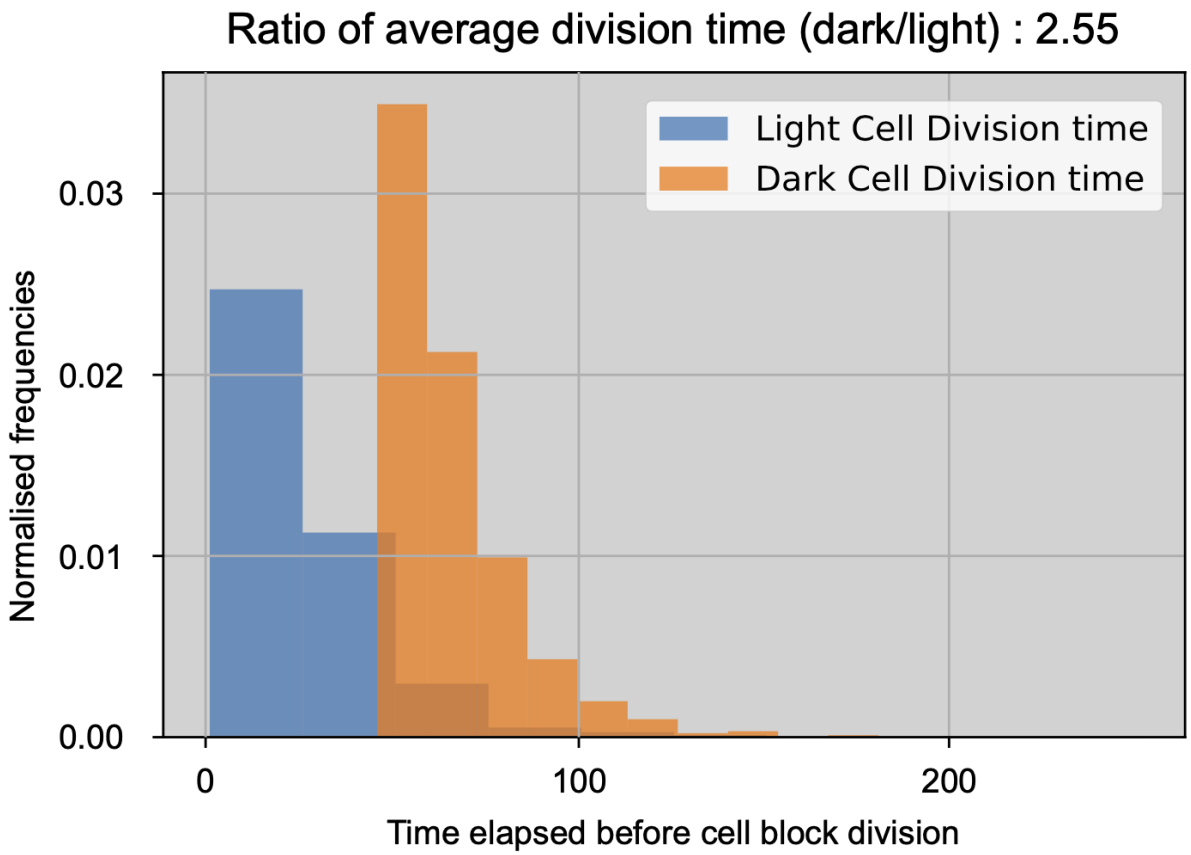

Figure 3-figure supplement 2: Normalized histograms of dark and light cell block division times through one simulation with default parameters. The bins along the x-axis measure the time steps elapsed between a cell block's birth and when it divides. The cell blocks have the same probability of division once they build up sufficient N and C reserves. These histograms illustrate that the division times in our simulation are different due to resource requirements being fulfilled at different times.

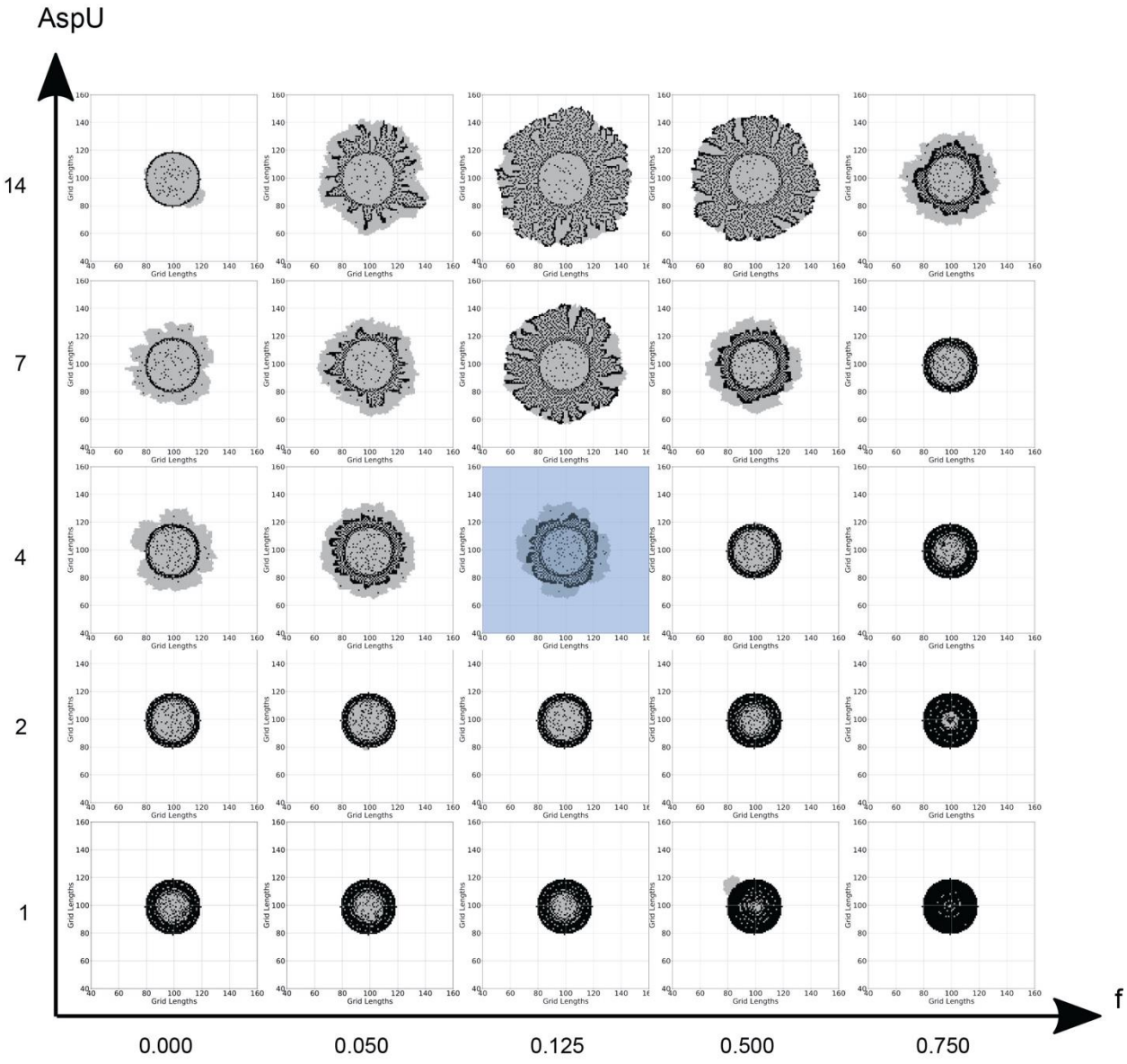

Figure 3-figure supplement 3: Different final colony compositions for different combinations of the main model parameters, 'f' and 'AspU'. Each panel is a generated colony using the values of 'f' and 'AspU' corresponding to its location. Note: the axes values are not on a linear or logarithmic scale but are for chosen for representative purposes to show parametric trends. Increasing AspU increases the rate of aspartate influx into the system. Overall, this generates larger colonies. Since dark cell blocks are not limited by the trehalose production, they divide at about the same rate as light cell blocks. This is contrary to experimental observations where dark cells grow slower than light cells. With the parameter f, extremely low values allocate too little of the metabolic budget to nitrogen reserves. This results in slow growing colonies which have a higher fraction of light cell blocks. On the other hand, higher values allocate too much of the budget to nitrogen reserves. This slows down the rate of trehalose production, thereby slowing down the emergence of light cells and their proliferation and gives us smaller overall colonies. Thus, increasing both AspU and f together leads to realistic looking colonies as observed along the top diagonal elements in this figure. The blue shaded central panel in the figure is a colony generated using default values of f and AspU.

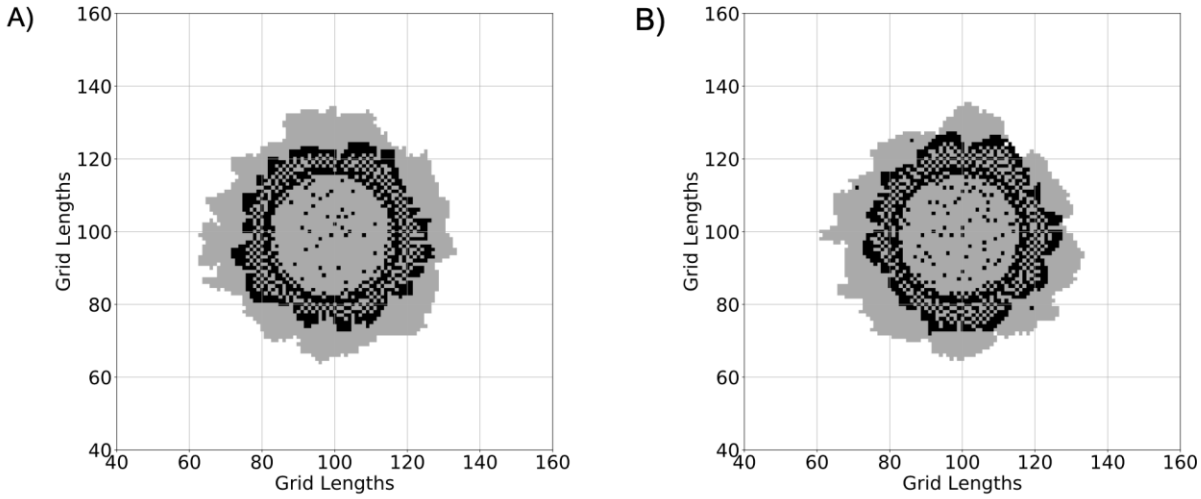

Figure 3-figure supplement 4:

(A) A colony where light cell blocks are not allowed to switch to dark cell blocks during the simulation. This is similar to the original model implemented in (Varahan et al., 2019).

(B) A colony implemented using our current model, where light cell blocks can switch to dark cell blocks with a low probability (p_{LD} = 10-4/Time), if the level of trehalose at their location is below a certain threshold (T_{LD} = 10-4 units). The two panels illustrate how the colonies are not significantly different, but the current model does not allow the light cells to remain fixed in their metabolic state.

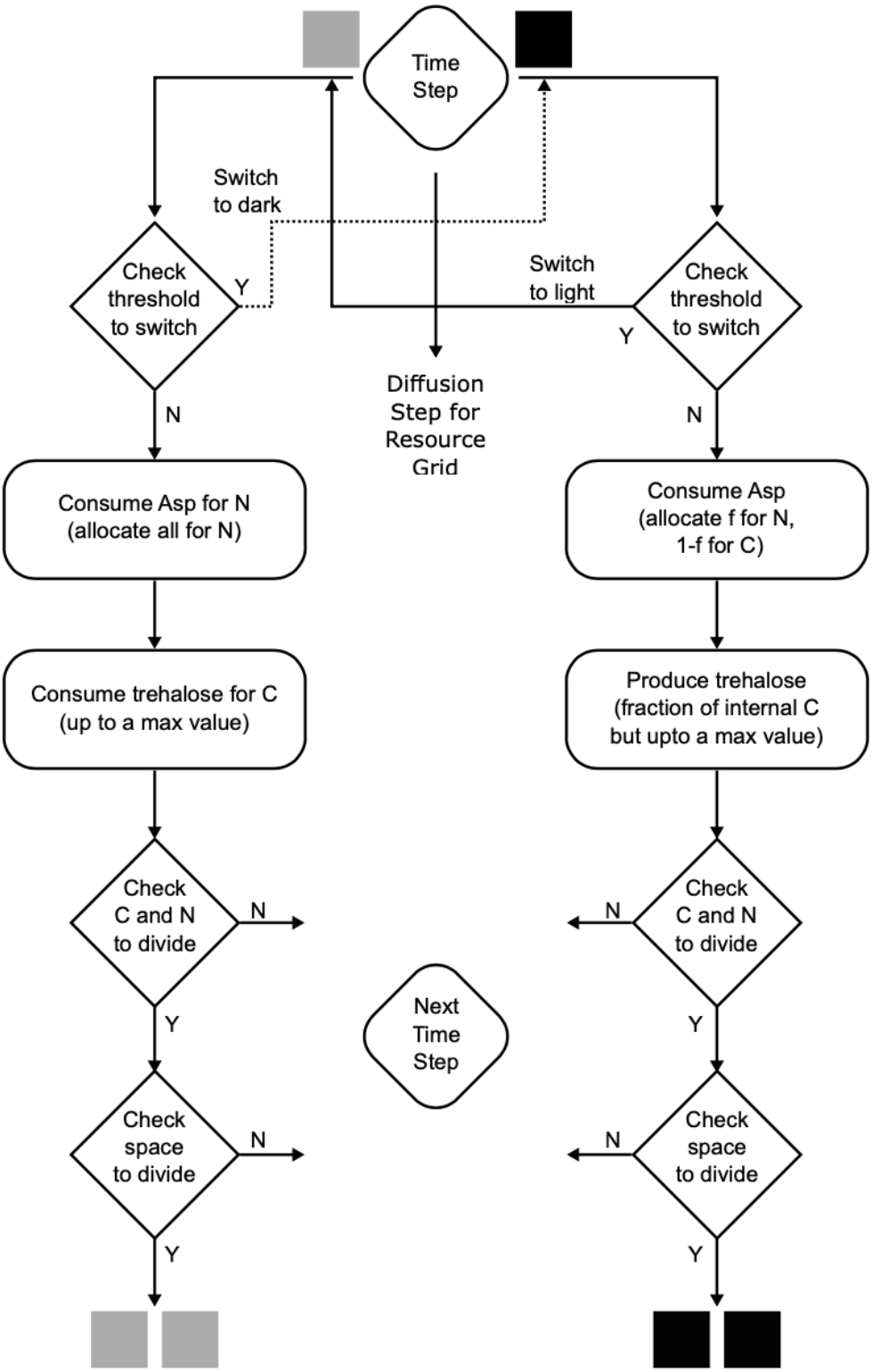

834

835 **Figure 3-figure supplement 5:** A flowchart of the simulation algorithm highlighting all the processes in
836 the mathematical model. A step-by-step description is provided in the Methods section of the main text.

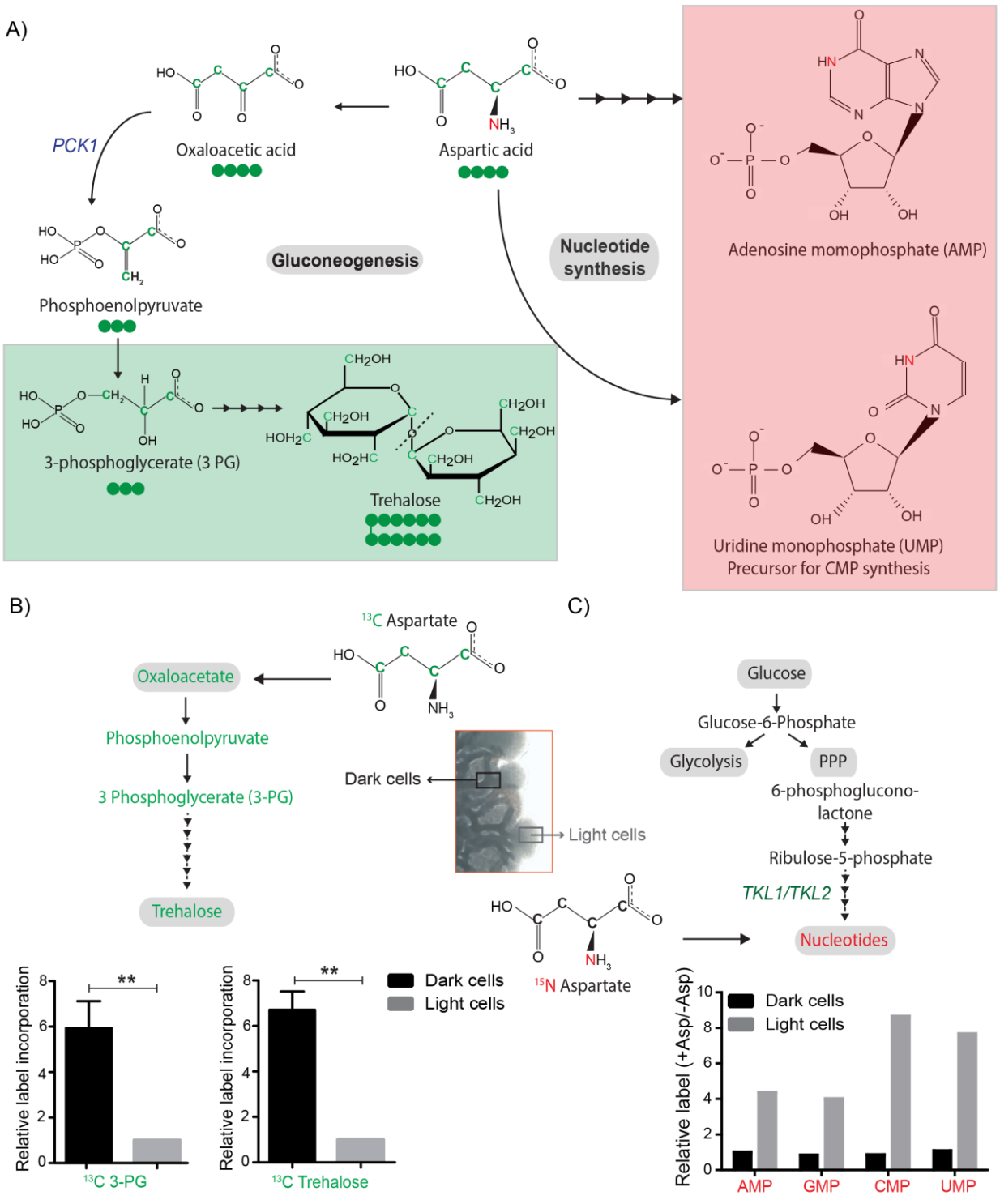

Figure 4. Aspartate is differentially utilized as a carbon or nitrogen currency in light and dark cells:

(A) Metabolic fates of aspartate: The carbon of aspartate (green) can be used for synthesis of molecules like trehalose *via* gluconeogenesis (Green boxed). The nitrogen of aspartate (red) is incorporated into nucleotide precursors including inositol monophosphate (IMP) AND cytidine monophosphate (CMP) (Red boxed).

(B) Comparative metabolic-flux based analysis comparing ^{13}C incorporation from ^{13}C labelled aspartate into newly synthesized gluconeogenic intermediate (3-phosphoglycerate) and trehalose and ^{15}N incorporation from ^{15}N labelled aspartate into newly synthesized nucleotides, in light and dark cells (n=3). Statistical significance was calculated using unpaired t test (** indicates $p<0.01$) and error bars represent standard deviation.

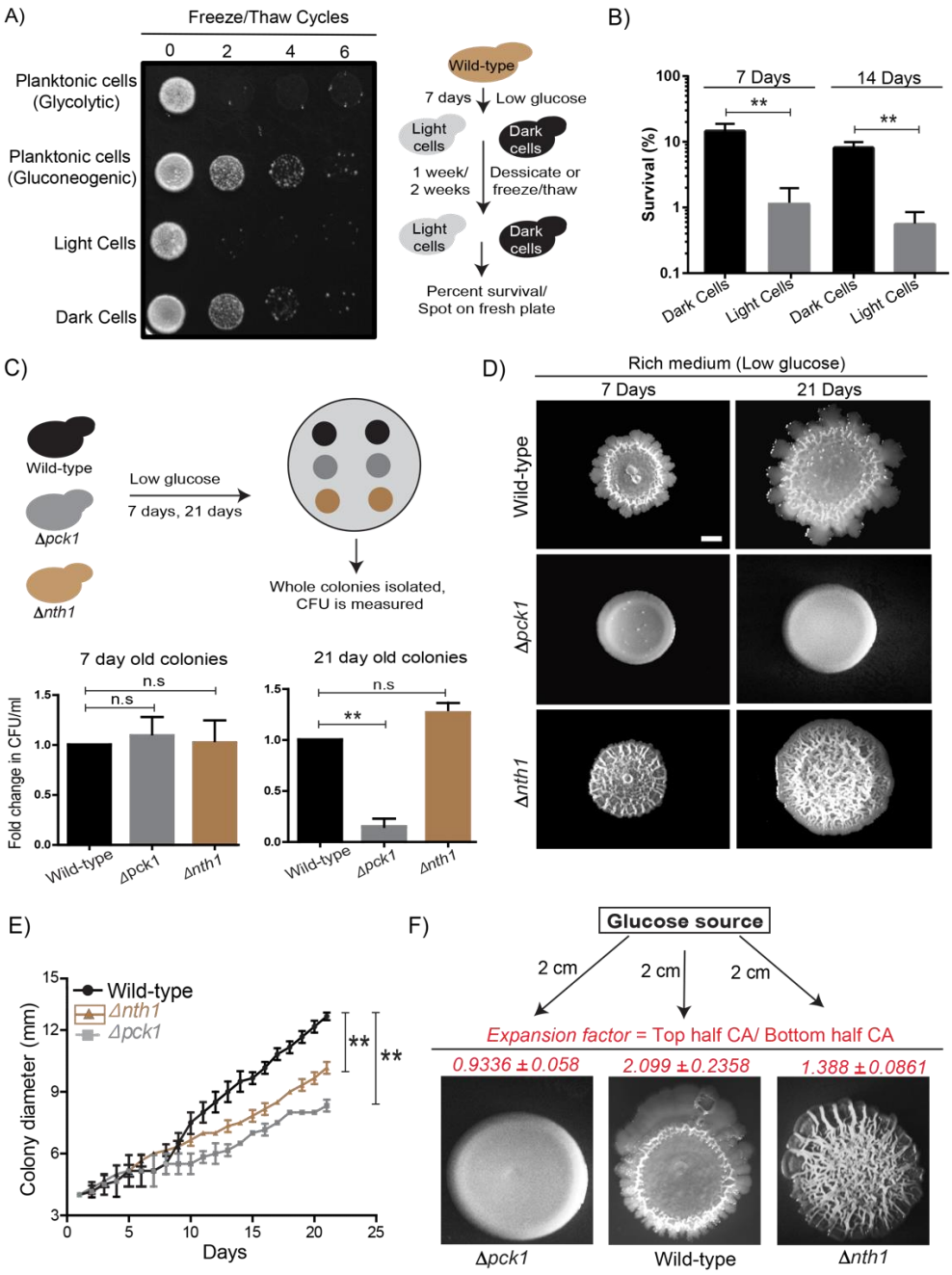

Figure 5. Dark and light cells exhibit division of labor by conferring distinct survival and collective growth advantages to the whole colony:

(A) Equal numbers of light and dark cells were subjected to multiple freeze-thaw cycles, and survival estimated by spotting onto rich media plates and allowing growth for 18 hours. Cells grown in gluconeogenic medium (2% ethanol/glycerol) and glycolytic medium (2% glucose) were used as controls.

858 **(B)** Desiccation tolerance of light and dark cells were measured after 7 days and 14 days (n=3). Statistical
859 significance was calculated using unpaired t test (** indicates p<0.01) and error bars represent standard
860 deviation.

861 **(C)** Long term viability of cells in wild-type (light and dark cells), Δ*nth1* (only dark cells) and Δ*pck1* (no
862 light or dark cells) colonies were measured by growing colonies for either 7 or 21 days and collecting cells
863 from the colonies and plating them in rich medium (n=5). Statistical significance was calculated using
864 unpaired t test (** indicates p<0.01) and error bars represent standard deviation.

865 **(D & E)** Foraging responses of wild-type, Δ*nth1* and Δ*pck1* cells measured as a function of their ability to
866 spread on a plate. Colony spreading was quantified by measuring the diameter of the colonies every day
867 for 21 days (n = 3). Statistical significance was calculated using unpaired t test (** indicates p<0.01) and
868 error bars represent standard deviation. Scale bar: 2mm.

869 **(F)** Directional foraging of light cells towards glucose was measure by growing wild-type cells, Δ*nth1* cells
870 and Δ*pck1* cells on rich medium plates (low glucose) and placing a paper disc soaked in 50% glucose at
871 a distance of 2 cm from the colonies (n=3).

872

873

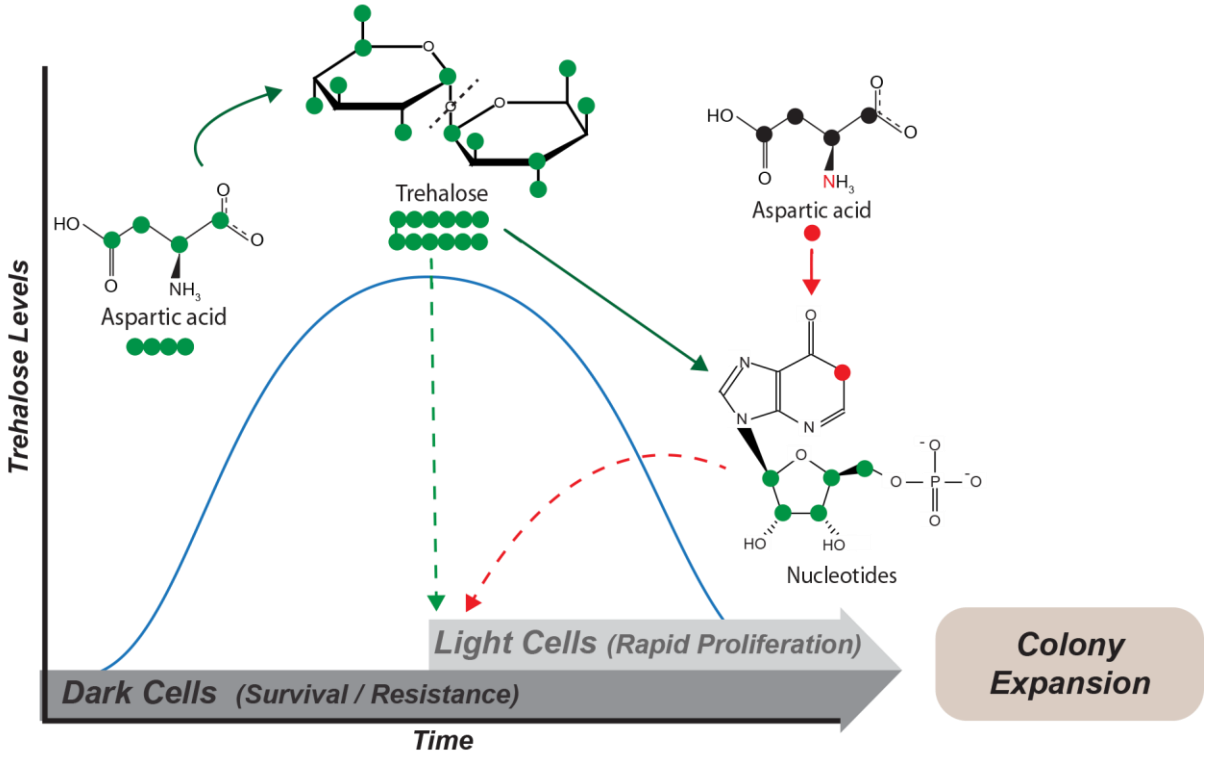

874

875 **Figure 6. Model: Carbon/Nitrogen resource budgeting of aspartate drives metabolic specialization**
876 **resulting in division of labor:** Cells in low glucose perform gluconeogenesis (Dark cells), as required in
877 low glucose medium. During this process, dark cells predominantly budget aspartate for their carbon
878 needs to synthesize trehalose. The accumulated trehalose reserves in the dark cells allow them to
879 survive environmental challenges including desiccation and repeated freeze/thaw cycles. Once threshold
880 levels of external trehalose are reached, some cells stochastically switch to the light state and utilize this
881 trehalose to fuel their high glycolysis and pentose phosphate pathway (PPP). Post this switch to the light
882 cell state, cells start using aspartate as a nitrogen source to synthesize nucleotides via PPP. This makes
883 light cells primed for proliferation, which in turn results in increased or directional colony expansion. This
884 division of labor between the light and dark cells allows the colony as a whole to survive unfavorable
885 conditions and forage efficiently even in nutrient limiting conditions.

886

887

888 **Video clip legends:**

889 **Video 1: Development of a simulated wild-type colony.** A simulation movie of the WT colony over 750
890 time-steps (~6 days in real time). The colony starts with 95-99% dark cells, which go through switching
891 and growth phases as observed. This colony is generated using default parameter values in the model.

892 **Video 2: Aspartate is allocated equally for Carbon and Nitrogen by dark cells.** A simulation movie
893 where the budgeting fraction 'f' is 50%, i.e., 50% of the aspartate flux is allocated towards nitrogen
894 reserves. The dark cell blocks cannot allocate sufficient carbon for themselves, leading to almost no
895 divisions by the dark cell blocks while the light cells at the edge keep proliferating. For comparison, the
896 default value of 'f' is 12.5%.

897 **Video 3: Aspartate uptake rate by both types of cells is equal to trehalose uptake rate by light**
898 **cells.** A simulation movie where the relative rate of aspartate uptake is equal to the trehalose uptake
899 rate. (i.e. AspU = 1.0). In this case, the aspartate uptake by dark cells is much slower, which also leads to
900 slower trehalose production, resulting in smaller colonies consisting of predominantly dark cell blocks.

901 **Video 4: Aspartate uptake rate by both types of cells is much higher than trehalose uptake rate by**
902 **light cells.** A simulation movie where the relative rate of aspartate uptake is high. (i.e. AspU = 8.0). In this
903 case, the dark cells allocate adequate aspartate for both nitrogen and carbon requirements rapidly
904 enough. This leads to both dark and light cells having nearly the same division rate.

905